

First measurement of $D_{s1}(1^+)(2536)^+$ and $D_{s2}^*(2^+)(2573)^+$ production in proton-proton collisions at $\sqrt{s}=13$ TeV at the LHC

S. Acharya *et al.*^{*}
(ALICE Collaboration)



(Received 21 October 2024; accepted 21 April 2025; published 16 June 2025)

The production yields of the orbitally excited charm-strange mesons $D_{s1}(1^+)(2536)^+$ and $D_{s2}^*(2^+)(2573)^+$ were measured for the first time in proton-proton (pp) collisions at a center-of-mass energy of $\sqrt{s}=13$ TeV with the ALICE experiment at the LHC. The D_{s1}^+ and D_{s2}^{*+} mesons were measured at midrapidity ($|y| < 0.5$) in minimum-bias and high-multiplicity pp collisions in the transverse-momentum interval $2 < p_T < 24$ GeV/ c . Their production yields relative to the D_s^+ ground-state yield were found to be compatible between minimum-bias and high-multiplicity collisions, as well as with previous measurements in $e^\pm p$ and e^+e^- collisions. The measured D_{s1}^+/D_s^+ and D_{s2}^{*+}/D_s^+ yield ratios are described by statistical hadronization models and can be used to tune the parameters governing the production of excited charm-strange hadrons in Monte Carlo generators, such as PYTHIA 8.

DOI: 10.1103/PhysRevD.111.112005

The production of charm mesons with spin zero (D mesons) or one (D^* mesons) and orbital angular momentum $L=0$ has been extensively studied in recent years in proton-proton (pp) collisions at the LHC by the ALICE [1–3], ATLAS [4], CMS [5], and LHCb [6,7] Collaborations. The production cross sections are generally described within uncertainties by perturbative QCD calculations at next-to-leading order (NLO) with next-to-leading log resummation (e.g., FONLL [8–10] and GM-VFNS [11,12]) via the factorization of three terms, namely the parton distribution functions (PDFs) of the incoming protons, the partonic cross section, and the fragmentation functions (FFs) describing the transition from charm quarks to the final hadrons. In these calculations, the FFs are typically parametrized from measurements in e^+e^- and $e^\pm p$ collisions [13] under the assumption that the hadronization of charm quarks into charm hadrons is a universal process, independent of the collision system. The relative abundances of the different D-meson species were found to be compatible with those measured in e^+e^- and $e^\pm p$ collisions [2,3]. A significant discrepancy was instead observed at midrapidity for the charm baryons, whose production relative to the one of the D^0 meson turned out to be enhanced in pp collisions compared to e^+e^- and $e^\pm p$ collisions [14–21], implying a modification of the

fragmentation fractions of charm quarks to the various charm-hadron species in pp collisions at LHC energies compared to those measured at lepton colliders at the LHC [3,22].

The charm-meson spectroscopy has also progressed significantly in the last few decades, with also the discovery of several excited charm and charm-strange states and the determination of their properties [23–31]. However, the production yields of charm resonances were only measured at e^+e^- and $e^\pm p$ colliders [32–35], and no experimental result is available in hadronic collisions. The knowledge about the production yields of such states would provide important information about the hadronization of charm quarks produced in hadronic collisions, since they contribute to the ground-state charm-hadron yields via strong decays. This is, for example, the case in models based on statistical hadronization, in which the yields of the various charm-hadron species are assumed to follow the relative thermal densities and hence depend on the state mass and spin-degeneracy factor $2J+1$, where J is the total angular momentum [36,37]. Charm resonances are typically not included in Monte Carlo (MC) generators, such as PYTHIA 8 [38], due to the lack of knowledge about their production and decays. Moreover, the production of short-lived resonances is important to study the hadronic phase of the system created in heavy-ion collisions. In the case when a resonance has a lifetime comparable to that of the hadronic phase, suppression or regeneration of the resonance state due to interactions of its decay products with the hadron gas is observed [39–42]. A lower limit of the lifetime of the hadronic phase in central Pb–Pb collisions of about 4–7 fm/ c was determined via the measurement of the p_T -integrated yield ratio of the

^{*}Full author list given at the end of the article.

$K^*(892)^0$ resonance ($c\tau \approx 4$ fm) to K^\pm mesons [39]. In addition, a hint of suppression was also measured in p–Pb and high-multiplicity pp collisions, suggesting the possible presence of rescattering effects and, thus, of a hadronic phase with a short but nonzero lifetime in small collision systems [40].

In this letter, the first measurement of the production yields of the orbitally excited charm-strange mesons $D_{s1}(1^+)(2536)^+$ ($c\tau \approx 214$ fm) and $D_{s2}^*(2^+)(2573)^+$ ($c\tau \approx 11.7$ fm) [43] and their charge conjugates in minimum-bias and high-multiplicity pp collisions at a center-of-mass energy of $\sqrt{s} = 13$ TeV is reported. In the following, D_{s1}^+ denotes $D_{s1}(1^+)(2536)^+$, and D_{s2}^{*+} stands for $D_{s2}^*(2^+)(2573)^+$. The results, which are integrated in the transverse-momentum interval $2 < p_T < 24$ GeV/ c where it was possible to observe a stable signal, are divided by the production yield of the ground state D_s^+ and compared with predictions obtained with the statistical hadronization model. The measured ratios are also used to constrain the parameters in PYTHIA 8, which regulate the production of pseudovector and tensor charm mesons, both with the inclusion of rescattering effects in the hadronic phase or without them. Finally, the excited-to-ground state yield ratios are exploited to compute the fragmentation fractions of charm quarks into the D_{s1}^+ and D_{s2}^{*+} states. The measured values are compared to those obtained in e^+e^- collisions.

The apparatus of the ALICE experiment and its performance during the Run 2 data-taking period are described in detail in Refs. [44] and [45]. The main subdetectors, located at midrapidity ($|y| < 0.5$), employed to perform the measurements presented in this letter are: the Inner Tracking System (ITS), for tracking and vertex reconstruction; the time projection chamber (TPC), for tracking and particle identification (PID); the time-of-flight (TOF) detector, for particle identification. The V0 detector, composed of two arrays of scintillators located on both sides of the collision region ($-3.7 < \eta < -1.7$ and $2.8 < \eta < 5.1$), is used for trigger purposes as well as to measure the event multiplicity [46]. The latter is determined from the percentile distribution of the summed amplitude recorded by both sides of the V0 detector, the V0M. Percentile values for higher multiplicity collisions are close to 0% and for lower ones close to 100%. In the following, the 0–0.1% V0M multiplicity class is denoted as HMV0.

The measurements reported in this paper were performed on the sample of pp collisions at $\sqrt{s} = 13$ TeV collected with the ALICE experiment from 2016 to 2018. The data were recorded using a minimum-bias trigger (MB) requiring coincident signals in both V0 scintillator arrays. Offline selection criteria were applied to remove beam-induced background events, exploiting the timing information from the V0 arrays and the correlation between the number of clusters and track segments reconstructed in the two innermost layers of the ITS. Events with pileup of

collisions within the same bunch crossing, with an estimated probability ranging from 10^{-3} to 10^{-2} depending on the beam conditions, were excluded by rejecting events with more than one reconstructed primary vertex [46]. To ensure uniform pseudorapidity acceptance, only events with a primary vertex position within ± 10 cm from the nominal center of the apparatus along the beam direction were considered. Furthermore, the events satisfying the aforementioned selection criteria were required to possess at least one reconstructed track segment between the first two layers of the ITS within $|\eta| < 1$ ($\text{INEL} > 0$ event class).

The resulting data sample consisted of about 1.8×10^9 $\text{INEL} > 0$ and 0.3×10^9 HMV0 events, corresponding to integrated luminosities of about 32 nb^{-1} and 7.7 pb^{-1} [47], respectively. The multiplicity percentile measured by the V0 detector was converted into an average charged-particle multiplicity, $\langle dN_{\text{ch}}/d\eta \rangle_{|\eta| < 0.5}$, by following the prescription detailed in Ref. [46]. A trigger correction was applied to account for those events that fulfill the $\text{INEL} > 0$ requirement but were not selected by the trigger. This correction factor $\epsilon^{\text{INEL}} = 0.920 \pm 0.003$ was estimated with a detailed Monte Carlo simulation based on the PYTHIA 8 generator [38] and the GEANT4 transport package [48]. For the HMV0 events the trigger was fully efficient and, therefore, a correction is not necessary [49].

The D_{s1}^+ and D_{s2}^{*+} mesons and their charge conjugates were measured at midrapidity through the hadronic decay channels $D_{s1}^+ \rightarrow D^{*+} K_S^0$ and $D_{s2}^{*+} \rightarrow D^+ K_S^0$, whose branching ratios (BRs) are not yet measured [43]. The K_S^0 mesons were reconstructed via $K_S^0 \rightarrow \pi^+ \pi^-$ decays with a BR of $(69.20 \pm 0.05)\%$ [43]. D^+ and D^{*+} mesons were reconstructed in the decay channels $D^+ \rightarrow K^- \pi^+ \pi^+$ with a BR of $(9.38 \pm 0.16)\%$ [43] and $D^{*+} \rightarrow D^0 (\rightarrow K^- \pi^+) \pi^+$ with a BR of $(2.67 \pm 0.03)\%$ [43], respectively. The reconstruction and selection of K_S^0 -meson candidates closely followed the approaches presented in previous publications [50,51]. Pairs of tracks with opposite charge signs, with $|\eta| < 0.8$ and satisfying the track-quality and particle-identification (PID) criteria reported in Ref. [50], were formed. Further selections based on the characteristic weak-decay topology of K_S^0 mesons were applied to reduce the combinatorial-background contribution. Similarly, D^0 - and D^+ -meson candidates were obtained from pairs and triplets of tracks, respectively, with the proper charge signs and $|\eta| < 0.8$. The D^{*+} -meson candidates were reconstructed by combining D^0 candidates with tracks identified as pions and having $p_T > 50$ MeV/ c . The signal selection exploited the reconstruction of decay-vertex topologies of D mesons displaced from the interaction vertex. A machine-learning approach based on boosted decision trees (BDTs) [52,53] was used to enhance the rejection of the combinatorial background and to separate D mesons produced directly in the charm-quark hadronization or

through decays of excited charm-hadron states (prompt) from those originating from beauty-hadron decays (non-prompt). The quantities provided as input to the BDTs were based on the topological and kinematic properties of the D-meson candidates, and the PID information of their daughter tracks. The selection procedure and criteria were the same as those used in Refs. [54] and [55], for D^+ and D^{*+} mesons respectively. D_{s1}^+ - and D_{s2}^{*+} -meson candidates were reconstructed by combining D^{*+} and D^+ mesons with K_S^0 mesons satisfying the aforementioned selection criteria. Furthermore, only D^{*+} , D^+ , and K_S^0 mesons with a reconstructed invariant mass within a window of $\pm 3\sigma$ around the reconstructed mass value were considered, where the signal-peak width (σ) and mean for the three meson species were estimated by fitting their particle-candidate invariant-mass distributions with a Gaussian plus a function to describe the combinatorial background. No additional requirements were applied to the orbitally excited charm-strange meson candidates.

The raw yields of D_{s1}^+ and D_{s2}^{*+} mesons were computed by integrating the signal function obtained from maximum-likelihood fits to the invariant-mass distributions $\Delta M = M(K\pi K_S^0) - M(K\pi\pi)$. The raw yields were extracted in the transverse-momentum interval $2 < p_T < 24 \text{ GeV}/c$ for both the $\text{INEL} > 0$ and HMV0 samples. The signal peak was modeled with a Voigt function, defined as the convolution of a Gaussian function and a Breit–Wigner function [56]. The widths, Γ , of the D_s^+ -meson resonances were fixed to their PDG values $\Gamma(D_{s1}^+) = (0.92 \pm 0.05) \text{ MeV}/c^2$ and $\Gamma(D_{s2}^{*+}) = (16.9 \pm 0.7) \text{ MeV}/c^2$ [43], while the Gaussian parameters are let free. For the D_{s1}^+ meson, the background was modeled with the function $a_0 \sqrt{\Delta M - m(K_S^0)} e^{a_1 [\Delta M - m(K_S^0)]}$, where $m(K_S^0)$ is the nominal rest mass of the K_S^0 meson, and a_0 and a_1 are free fit parameters. A polynomial of first order was used to describe the background in the D_{s2}^{*+} -meson fits. The invariant-mass distributions are reported in Fig. 1 together with related fit functions. A statistically reliable signal extraction is obtained for both the D_{s1}^+ and D_{s2}^{*+} mesons for $\text{INEL} > 0$ and HMV0 events. The statistical significance, computed in the invariant mass region within three half-width half-maximum (HWHM) around the signal peak, ranges between 4.0 and 5.7 depending on the particle and multiplicity interval.

The corrected per-event yields times BR of prompt D_{s1}^+ and D_{s2}^{*+} mesons at midrapidity were computed for each multiplicity class as

$$\frac{1}{N^{\text{ev}}} \frac{d^2N}{dp_T dy} \times \text{BR} = \frac{1}{2} \frac{\epsilon^{\text{INEL}}}{N^{\text{ev}}} \frac{1}{\text{BR}(D) \times \text{BR}(K_S^0)} \\ \times \frac{f_{\text{prompt}} \times N^{\text{raw}}|_{|y| < y_{\text{lab}}}}{\Delta y_{\text{lab}} \times \Delta p_T \times (\text{Acc} \times \epsilon)_{\text{prompt}}}, \quad (1)$$

where N^{raw} is the raw yield, summed for particles and antiparticles, extracted in a given multiplicity class. The raw yield is divided by the prompt acceptance-times-efficiency $(\text{Acc} \times \epsilon)_{\text{prompt}}$ and multiplied by the fraction of prompt D mesons in the selected sample f_{prompt} to correct for the contribution of beauty-hadron decays. It is further divided by a factor of two to obtain the charge-averaged yield, by the p_T -interval width Δp_T , and by the correction factor accounting for the rapidity coverage of reconstructed excited charm-strange mesons Δy_{lab} . The term $\text{BR}(D) \times \text{BR}(K_S^0)$ encompasses the normalization for the decay-channel branching ratios of the D_s^+ -meson resonance daughters. The factor N^{ev} denotes the number of recorded events in the $\text{INEL} > 0$ multiplicity class. It is corrected for the fraction of $\text{INEL} > 0$ events that were selected by the trigger ϵ^{INEL} .

No kinematic selections were applied on the reconstructed D_{s1}^+ - and D_{s2}^{*+} -meson candidates. Therefore the prompt acceptance-times-efficiency corrections for D^{*+} , D^+ , and K_S^0 mesons were estimated as a function of p_T , y , and azimuthal angle from full MC simulations, in which pp collisions are simulated using the PYTHIA 8.243 event generator [57,58], the generated particles are propagated through the apparatus using GEANT4 [48] reproducing the detector layout and data-taking conditions, and the reconstruction of events is performed as in real data. They were then combined, in a second step, to obtain the $(\text{Acc} \times \epsilon)_{\text{prompt}}$ factor of D_{s1}^+ and D_{s2}^{*+} mesons using a fast MC simulation based on the PYTHIA 8.243 decayer to describe the excited charm-strange meson decay kinematics. In this case, the D_{s1}^+ and D_{s2}^{*+} mesons were sampled from the measured p_T distributions of D_s^+ mesons in the same multiplicity classes taken from Ref. [49] and let decay by the PYTHIA 8 decayer. The efficiency was then computed by evaluating it as the product of the efficiencies of the daughter particles as a function of p_T , η , and charged-particle multiplicity estimated in number of track segments reconstructed with the first two layers of the ITS. This approach was validated by estimating the efficiency corrections of D_{s1}^+ and D_{s2}^{*+} mesons using a full MC simulation with a limited number of generated events. The results of the two methods were in agreement within uncertainties.

The D_s^+ -resonance prompt fraction f_{prompt} was computed from the one of D^{*+} and D^+ mesons by accounting for the decay kinematics with an approach similar to that for the $\text{Acc} \times \epsilon$ factor. The D-meson f_{prompt} was estimated with the data-driven method introduced in Ref. [2]. More details on the procedure and the obtained values can be found in Ref. [54] for D^+ mesons and Ref. [55] for D^{*+} mesons. A correction factor of 1.93 ± 0.37 was also applied to account for the higher probability of strange quarks contained in the D_{s1}^+ and D_{s2}^{*+} mesons to hadronise into a beauty rather than a charm hadron, as shown in Ref. [59]. This factor was obtained from the measurement

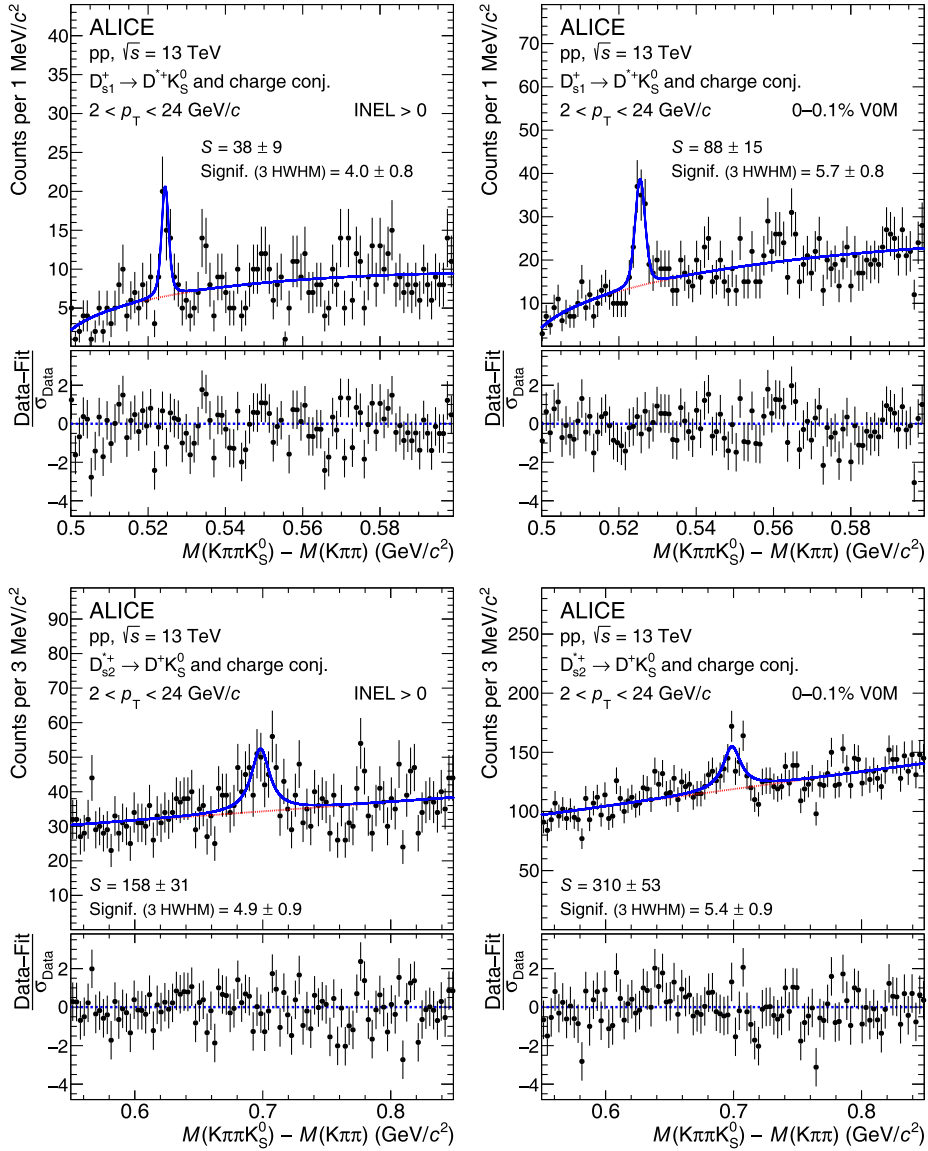


FIG. 1. Invariant-mass distributions $M(K\pi\pi K_S^0) - M(K\pi\pi)$ of D_s^+ (top panels) and D_s^{*+} (bottom panels) candidates and charge conjugates in the $2 < p_T < 24 \text{ GeV}/c$ interval, for the $\text{INEL} > 0$ and HMV0 ($0-0.1\%$ V0M) samples. The blue solid lines show the total fit functions described in the text, and the red dashed lines represent the combinatorial background. The raw-yield (S) values are reported together with their statistical uncertainties, as well as the estimated significance of the signal (Signif.). The bottom subpanels of each panel display the differences between the data and the fit, normalized by the experimental uncertainties, to show the agreement between the data and the fit.

of prompt and nonprompt strange and nonstrange D mesons in pp collisions at $\sqrt{s} = 13 \text{ TeV}$ [3,59]. The resulting prompt fraction of D_s^+ (D_s^{*+}) mesons is larger than 0.75 (0.85) in both the HMV0 and $\text{INEL} > 0$ samples.

The systematic uncertainties on the corrected yields of the measured D_s^+ -meson resonances in both the $\text{INEL} > 0$ and HMV0 samples include the following sources: (i) extraction of the raw yield, (ii) prompt-fraction estimation, (iii) tracking and selection efficiency evaluation, (iv) sensitivity of the efficiencies to the meson p_T shape generated in the simulation and (v) to the description of the

charged-particle multiplicity. In addition, an overall normalization systematic uncertainty due to uncertainties in the BR and the integrated luminosity was considered.

The systematic uncertainty on the raw-yield extraction was assessed by repeating the yield extraction after varying the fit configuration, in particular the fit ranges, the fit function used to describe the background, and the value of the Γ parameter by accounting for its uncertainty as reported in Ref. [43]. The systematic uncertainties related to the estimation of the prompt resonance fraction in the extracted yields were computed by varying the reference

value of the strange-to-nonstrange D-meson ratio within the range of its uncertainties. The magnitude of these uncertainties depends on the multiplicity class and ranges between 5% and 14% for the D_{s1}^+ , and between 4% and 7% for the D_{s2}^{*+} , respectively.

The systematic uncertainty on the track-reconstruction and selection efficiencies accounts for possible discrepancies between data and MC in the ITS–TPC prolongation, track-quality selection efficiency, description of the ALICE detector material budget, and description of the topological and PID variables exploited for the K_S^0 and D-meson selection. The track-reconstruction systematic uncertainty was estimated by propagating the track-reconstruction systematic uncertainty on the single decay daughter track to the resonance considering the kinematic of the decay. The systematic on the selection efficiency was assessed by repeating the measurement of the D_{s1}^+ and D_{s2}^{*+} corrected yields after varying the selection criteria applied to the K_S^0 and D mesons. The magnitude of the systematic uncertainty related to the tracking and the BDT efficiency for both D_s^+ states is of 6% and 10%, respectively.

The systematic uncertainties associated with the description of the p_T shape and the multiplicity of the events in the simulation were evaluated by varying the functional form employed to describe the p_T distribution of the generated resonances and by repeating the study employing different multiplicity weights accounting for different event-selection criteria. The assigned systematic uncertainty associated with the p_T shape varies between 10 and 13% depending on the multiplicity class for both the

D_s^+ states. The uncertainty associated with the multiplicity is less than 2% for both D_s^+ states.

The ratios of the yields of the D_{s1}^+ and D_{s2}^{*+} mesons times the relative BRs to that of the D_s^+ meson as a function of the average charged-particle multiplicity $\langle dN_{ch}/d\eta \rangle_{|\eta|<0.5}$ at midrapidity in pp collisions at $\sqrt{s} = 13$ TeV are shown in Fig. 2. The p_T -differential measurements of the D_s^+ -meson yields performed by the ALICE Collaboration for the INEL > 0 [3] and HMV0 [49] multiplicity classes, integrated over the p_T range between 2 and 24 GeV/ c , were used as the denominators of the ratios. The systematic uncertainties associated with the corrected yields were treated as uncorrelated in the propagation to the ratios, except the one related to the luminosity, which was treated as fully correlated and cancels out in the ratio. The statistical and systematic uncertainties are depicted as vertical lines and empty boxes, respectively. The ratios do not show a significant dependence on $\langle dN_{ch}/d\eta \rangle_{|\eta|<0.5}$.

The measurements were compared with the predictions based on the statistical hadronization model (SHM) [37] and the SHM for charm hadrons (SHMc) of the GSI–Heidelberg group [60], integrated over $p_T > 0$, and with the predictions from EPOS4HQ [61] in two different configurations. In the SHM and SHMc, hadron abundances are dictated by thermal weights depending on the hadron rest masses. Both the SHM and SHMc include a set of not yet observed charm-baryon states. However, unlike the SHM, SHMc assumes that charm quarks are produced in initial hard scattering processes and that the total number of (anti)charm quarks is conserved in the collision.

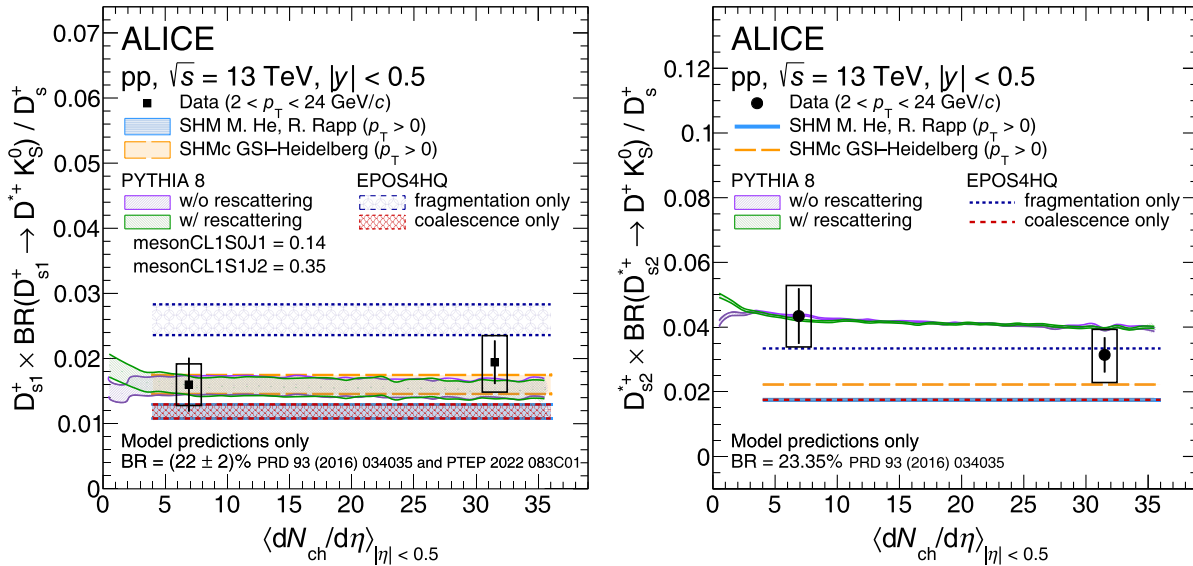


FIG. 2. D_{s1}^+/D_s^+ (left) and D_{s2}^{*+}/D_s^+ (right) ratio times BR as a function of the average charged-particle multiplicity $\langle dN_{ch}/d\eta \rangle_{|\eta|<0.5}$ in pp collisions at $\sqrt{s} = 13$ TeV at midrapidity ($|y| < 0.5$). The experimental results are compared with the theoretical predictions based on the SHM [37], the SHMc [60], PYTHIA 8 [57,58], and EPOS4HQ [61]. The statistical and systematic uncertainties on the measured ratios are depicted as vertical lines and boxes, respectively. The theoretical uncertainty on the predicted ratios is depicted as a shaded band for the D_{s1}^+ .

Computing the ratio between the excited- and ground-state charm hadron yields is beneficial for the theoretical predictions as the dependency on strangeness and charm corrections cancel out exactly. The EPOS4HQ is the heavy hadron extension of the EPOS4 generator [62]. Heavy flavor quarks, produced in hard scatterings, gluon splittings, or flavor excitation, may interact with the medium constituents through elastic and inelastic processes and finally hadronize via fragmentation or coalescence. The two mechanisms are complementary and dominate at high and low momenta, respectively. The SHM, SHMc, and EPOS4HQ predictions necessitate being scaled by the BR of the analyzed hadronic decay to be fairly compared with the measurements. No measurement of these BRs is currently available, thus they were computed considering the predictions of the BR of the $D_{s1}^+ \rightarrow D^* K$ and $D_{s2}^{*+} \rightarrow DK$ decays from the relativistic quark model (RQM) [63] and the ratio of the BRs between the two possible final charged states. The SHM and EPOS4HQ in the pure coalescence configuration completely overlap in both the D_{s1}^+/D_s^+ and D_{s2}^{*+}/D_s^+ cases. In the case of the D_{s1}^+ , the value reported by the PDG [43] was used with its uncertainty, while in the case of the D_{s2}^{*+} an equal contribution to $D_{s2}^{*+} \rightarrow D^+ K^0$ and $D_{s2}^{*+} \rightarrow D^0 K^+$ was assumed, given the very similar Q-values of the decays. The resulting values are: $\text{BR}(D_{s1}^+ \rightarrow D^{*+} K_S^0) = (22 \pm 2)\%$ and $\text{BR}(D_{s2}^{*+} \rightarrow D^+ K_S^0) = 23.35\%$ for the D_{s1}^+ and D_{s2}^{*+} , respectively. The uncertainties associated with the computed BR, incorporating the uncertainties on the branching fraction provided by the PDG when available, were extended to the theoretical predictions and are depicted as shaded regions for the D_{s1}^+ . The theoretical predictions from the SHM and the SHMc for the D_{s1}^+/D_s^+ ratio are flat as a function of multiplicity and in good agreement with the measured ratios within 0.5 and 1.2σ at high and low multiplicity, respectively. They slightly underestimate the measured central values of the D_{s2}^{*+}/D_s^+ ratio by 2σ and 1σ at low and high multiplicity, respectively. The experimental results are also compared with predictions from EPOS4HQ considering pure fragmentation or coalescence, respectively. The predicted ratios are systematically lower in the case of pure coalescence compared to pure fragmentation. A more realistic description including both the hadronization mechanisms would provide a prediction in between the ones reported in Fig. 2, therefore more in agreement with the measured ratios. The comparison with the model predictions align with what was observed for the ratio of ground-state charm mesons in pp collisions at the LHC energies [3,22] indicating that a quantitative description of the relative production of charm meson states is successfully achieved using a statistical approach.

Orbitally excited states like the D_{s1}^+ and D_{s2}^{*+} mesons are not considered in the PYTHIA 8 generator by default. Nevertheless, they can be included in the generation with

a parametrized description of their production and subsequent decay. The parameters regulating the production of pseudovector and tensor charm mesons (i.e., mesonCL1S0J1 and mesonCL1S1J2) were tuned to minimize the χ^2 between the measured excited-to-ground state ratio in the $\text{INEL} > 0$ sample and the predicted one from PYTHIA 8, obtaining $\text{mesonCL1S0J1} = 0.14$ and $\text{mesonCL1S1J2} = 0.35$. In the simulation, the average charged-particle multiplicity was estimated considering the multiplicity of charged tracks at midrapidity. For the D_{s1}^+ , the uncertainty associated with the BR relative to the considered hadronic decay channel was propagated to the PYTHIA 8 predictions as done for the thermal models and is depicted as a shaded band. In the case of the D_{s2}^{*+}/D_s^+ ratio, the data points suggest a possible decrease with increasing $\langle dN_{\text{ch}}/d\eta \rangle_{|\eta|<0.5}$, even if the values for $\text{INEL} > 0$ and HMV0 are compatible within uncertainties. To investigate the possible effect of the hadronic rescattering on the dependence of these ratios on $\langle dN_{\text{ch}}/d\eta \rangle_{|\eta|<0.5}$, the PYTHIA 8 simulation was performed with and without enabling it [64]. The two configurations produce compatible results in the considered multiplicity range. This might be related to the fact that the lifetime of the D_{s2}^{*+} is longer than the expected duration of the hadronic phase in the collision and to the fact that the magnitude of hadronic interactions for D mesons with light hadrons is expected to be small in high-multiplicity pp collisions, as recently reported by the ALICE Collaboration [65,66].

The ratios presented above can be compared with those from measurements of the fragmentation fractions of charm quarks into D_{s1}^+ , D_{s2}^{*+} , and D_s^+ mesons ($f_c \rightarrow h_c$) performed in e^+e^- and $e^\pm p$ collisions at LEP [32–34,67]. The D_{s1}^+/D_s^+ and D_{s2}^{*+}/D_s^+ ratios were computed as $(f_c \rightarrow D_{s1}^+) / (f_c \rightarrow D_s^+)$ and $(f_c \rightarrow D_{s2}^{*+}) / (f_c \rightarrow D_s^+)$, respectively. A direct comparison of the ratios of the fragmentation fractions with the results presented in Fig. 2 cannot be made without first accounting for the BR of the decay of the resonance. The results shown in Fig. 2 were divided by the BR computed following the procedure discussed above. Figure 3 shows a compilation of the D_{s1}^+/D_s^+ and D_{s2}^{*+}/D_s^+ ratios along with the SHM predictions in pp collisions presented above. The uncertainty associated with the BR for the D_{s1}^+ is depicted separately as a shaded box. The ratios measured in pp collisions at the LHC and presented in this letter are consistent with those measured at LEP in e^+e^- and $e^\pm p$ collisions with a maximum deviation of 2.1σ for D_{s1}^+/D_s^+ in the $\text{INEL} > 0$ sample.

In summary, the production yields of $D_{s1}(1^+)(2536)^+$ and $D_{s2}^*(2^+)(2573)^+$ mesons were measured for the first time at the LHC in pp collisions at $\sqrt{s} = 13$ TeV in two classes of charged-particle multiplicity. Given the absence of measurements for the BR of the considered hadronic decay channels, the results were not corrected for the relative BR. The measurements were performed at

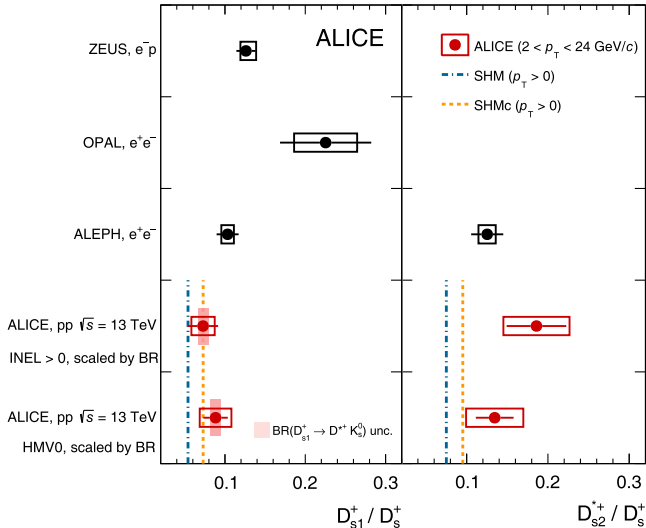


FIG. 3. p_T -integrated yields of prompt D_{s1}^+ (left) and D_{s2}^{*+} (right) mesons divided by the p_T -integrated yields of prompt D_s^+ mesons. The measurements are compared to the ones performed at LEP [32–34,67]. For the ALICE measurements, the results consider the BR of the decay of interest computed as described in the text considering the RQM [63] predictions and PDG information [43]. The experimental results are compared with the theoretical predictions based on the SHM [37] and the SHMc [60] models.

midrapidity in the $2 < p_T < 24 \text{ GeV}/c$ range, and the ratios to the analogous measurement for the D_s^+ mesons scaled by the BR of the hadronic decay channel of the resonances are reported. The excited-to-ground state ratios do not show any significant dependence on the multiplicity given the current experimental uncertainty. The measurements were compared with the predictions from SHM, SHMc, and EPOS4HQ models, which quantitatively describe them.

The measured ratios were also used to tune the parameters of the PYTHIA 8 event generator governing the production of these orbitally excited states. In particular, these parameters were set to optimize the agreement between the measurements and the predictions from PYTHIA 8 at lower multiplicity. To further test the possible effects of hadronic rescattering on the excited-to-ground state ratios, the PYTHIA 8 simulation was performed including this effect or not. However, no significant difference was found between the two configurations.

Finally, a comparison was made between the D_{s1}^+/D_s^+ and D_{s2}^{*+}/D_s^+ ratios presented in this letter and the ratios of the charm-quark fragmentation fractions measured at LEP in e^+e^- and $e^\pm p$ collisions. The results obtained at LHC and LEP are consistent within uncertainties. The extensive dataset collected during the Run 3 and 4 data-taking periods at the LHC will significantly reduce the relative uncertainties associated with these measurements, enabling a better understanding of the resonance production mechanism.

The ALICE Collaboration would like to thank all its engineers and technicians for their invaluable contributions to the construction of the experiment and the CERN accelerator teams for the outstanding performance of the LHC complex. The ALICE Collaboration gratefully acknowledges the resources and support provided by all Grid centers and the Worldwide LHC Computing Grid (WLCG) collaboration. The ALICE Collaboration acknowledges the following funding agencies for their support in building and running the ALICE detector: A. I. Alikhanyan National Science Laboratory (Yerevan Physics Institute) Foundation (ANSL), State Committee of Science and World Federation of Scientists (WFS), Armenia; Austrian Academy of Sciences, Austrian Science Fund (FWF): [M 2467-N36] and Nationalstiftung für Forschung, Technologie und Entwicklung, Austria; Ministry of Communications and High Technologies, National Nuclear Research Center, Azerbaijan; Conselho Nacional de Desenvolvimento Científico e Tecnológico (CNPq), Financiadora de Estudos e Projetos (Finep), Fundação de Amparo à Pesquisa do Estado de São Paulo (FAPESP) and Universidade Federal do Rio Grande do Sul (UFRGS), Brazil; Bulgarian Ministry of Education and Science, within the National Roadmap for Research Infrastructures 2020-2027 (object CERN), Bulgaria; Ministry of Education of China (MOEC), Ministry of Science & Technology of China (MSTC) and National Natural Science Foundation of China (NSFC), China; Ministry of Science and Education and Croatian Science Foundation, Croatia; Centro de Aplicaciones Tecnológicas y Desarrollo Nuclear (CEADEN), Cubaenergía, Cuba; Ministry of Education, Youth and Sports of the Czech Republic, Czech Republic; The Danish Council for Independent Research | Natural Sciences, the VILLUM FONDEN and Danish National Research Foundation (DNRF), Denmark; Helsinki Institute of Physics (HIP), Finland; Commissariat à l’Energie Atomique (CEA) and Institut National de Physique Nucléaire et de Physique des Particules (IN2P3) and Centre National de la Recherche Scientifique (CNRS), France; Bundesministerium für Bildung und Forschung (BMBF) and GSI Helmholtzzentrum für Schwerionenforschung GmbH, Germany; General Secretariat for Research and Technology, Ministry of Education, Research and Religions, Greece; National Research, Development and Innovation Office, Hungary; Department of Atomic Energy Government of India (DAE), Department of Science and Technology, Government of India (DST), University Grants Commission, Government of India (UGC) and Council of Scientific and Industrial Research (CSIR), India; National Research and Innovation Agency—BRIN, Indonesia; Istituto Nazionale di Fisica Nucleare (INFN), Italy; Japanese Ministry of Education, Culture, Sports, Science and Technology (MEXT) and Japan Society for the Promotion of Science (JSPS) KAKENHI,

Japan; Consejo Nacional de Ciencia (CONACYT) y Tecnología, through Fondo de Cooperación Internacional en Ciencia y Tecnología (FONCICYT) and Dirección General de Asuntos del Personal Académico (DGAPA), Mexico; Nederlandse Organisatie voor Wetenschappelijk Onderzoek (NWO), Netherlands; The Research Council of Norway, Norway; Pontificia Universidad Católica del Perú, Peru; Ministry of Science and Higher Education, National Science Centre and Warsaw University of Technology (WUT) ID-UB, Poland; Korea Institute of Science and Technology Information and National Research Foundation of Korea (NRF), Republic of Korea; Ministry of Education and Scientific Research, Institute of Atomic Physics, Ministry of Research and Innovation and Institute of Atomic Physics and Universitatea Națională de Știință și Tehnologie Politehnica Bucuresti, Romania; Ministry of Education, Science, Research and Sport of the Slovak Republic, Slovakia; National Research Foundation of South Africa, South Africa; Swedish Research Council (VR) and Knut & Alice Wallenberg Foundation (KAW), Sweden; European Organization for Nuclear Research, Switzerland; Suranaree University of Technology (SUT), National Science and Technology Development Agency (NSTDA) and National Science,

Research and Innovation Fund (NSRF via PMU-B B05F650021), Thailand; Turkish Energy, Nuclear and Mineral Research Agency (TENMAK), Turkey; National Academy of Sciences of Ukraine, Ukraine; Science and Technology Facilities Council (STFC), United Kingdom; National Science Foundation of the United States of America (NSF) and United States Department of Energy, Office of Nuclear Physics (DOE NP), United States of America. In addition, individual groups or members have received support from: Czech Science Foundation (Grant No. 23-07499S), Czech Republic; FORTE project, Reg. No. CZ.02.01.01/00/22_008/0004632, Czech Republic, cofunded by the European Union, Czech Republic; European Research Council (Grant No. 950692), European Union; ICSC—Centro Nazionale di Ricerca in High Performance Computing, Big Data and Quantum Computing, European Union—NextGenerationEU; Academy of Finland (Center of Excellence in Quark Matter) (Grant No. 346327 and No. 346328), Finland.

DATA AVAILABILITY

The data that support the findings of this article are openly available [68].

-
- [1] S. Acharya *et al.* (ALICE Collaboration), Measurement of D^0 , D^+ , D^{*+} and D_s^+ production in pp collisions at $\sqrt{s} = 5.02$ TeV with ALICE, *Eur. Phys. J. C* **79**, 388 (2019).
- [2] S. Acharya *et al.* (ALICE Collaboration), Measurement of beauty and charm production in pp collisions at $\sqrt{s} = 5.02$ TeV via non-prompt and prompt D mesons, *J. High Energy Phys.* **05** (2021) 220.
- [3] S. Acharya *et al.* (ALICE Collaboration), Charm production and fragmentation fractions at midrapidity in pp collisions at $\sqrt{s} = 13$ TeV, *J. High Energy Phys.* **12** (2023) 086.
- [4] G. Aad *et al.* (ATLAS Collaboration), Measurement of $D^{*\pm}$, D^\pm and D_s^\pm meson production cross sections in pp collisions at $\sqrt{s} = 7$ TeV with the ATLAS detector, *Nucl. Phys.* **B907**, 717 (2016).
- [5] A. Tumasyan *et al.* (CMS Collaboration), Measurement of prompt open-charm production cross sections in proton-proton collisions at $\sqrt{s} = 13$ TeV, *J. High Energy Phys.* **11** (2021) 225.
- [6] R. Aaij *et al.* (LHCb Collaboration), Measurements of prompt charm production cross-sections in pp collisions at $\sqrt{s} = 13$ TeV, *J. High Energy Phys.* **03** (2016) 159; **09** (2016) 013(E); **05** (2017) 074(E).
- [7] R. Aaij *et al.* (LHCb Collaboration), Measurements of prompt charm production cross-sections in pp collisions at $\sqrt{s} = 5$ TeV, *J. High Energy Phys.* **06** (2017) 147.
- [8] M. Cacciari, M. Greco, and P. Nason, The p_T spectrum in heavy flavor hadroproduction, *J. High Energy Phys.* **05** (1998) 007.
- [9] M. Cacciari, S. Frixione, and P. Nason, The p_T spectrum in heavy flavor photoproduction, *J. High Energy Phys.* **03** (2001) 006.
- [10] M. Cacciari, S. Frixione, N. Houdeau, M. L. Mangano, P. Nason, and G. Ridolfi, Theoretical predictions for charm and bottom production at the LHC, *J. High Energy Phys.* **10** (2012) 137.
- [11] B. A. Kniehl, G. Kramer, I. Schienbein, and H. Spiesberger, Inclusive Charmed-Meson Production at the CERN LHC, *Eur. Phys. J. C* **72**, 2082 (2012).
- [12] I. Helenius and H. Paukkunen, Revisiting the D -meson hadroproduction in general-mass variable flavour number scheme, *J. High Energy Phys.* **05** (2018) 196.
- [13] E. Braaten, K. Cheung, S. Fleming, and T. C. Yuan, Perturbative QCD fragmentation functions as a model for heavy quark fragmentation, *Phys. Rev. D* **51**, 4819 (1995).
- [14] S. Acharya *et al.* (ALICE Collaboration), Λ_c^+ production and baryon-to-meson ratios in pp and $p - \text{Pb}$ Collisions at $\sqrt{s_{\text{NN}}} = 5.02$ TeV at the LHC, *Phys. Rev. Lett.* **127**, 202301 (2021).
- [15] S. Acharya *et al.* (ALICE Collaboration), Λ_c^+ production in pp and in $p - \text{Pb}$ collisions at $\sqrt{s_{\text{NN}}} = 5.02$ TeV, *Phys. Rev. C* **104**, 054905 (2021).

- [16] S. Acharya *et al.* (ALICE Collaboration), Measurement of prompt D^0 , Λ_c^+ , and $\Sigma_c^{0,+}(2455)$ production in proton-proton collisions at $\sqrt{s} = 13$ TeV, *Phys. Rev. Lett.* **128**, 012001 (2022).
- [17] S. Acharya *et al.* (ALICE Collaboration), Measurement of the production cross section of prompt Ξ_c^0 baryons at midrapidity in pp collisions at $\sqrt{s} = 5.02$ TeV, *J. High Energy Phys.* **10** (2021) 159.
- [18] S. Acharya *et al.* (ALICE Collaboration), Measurement of the cross sections of Ξ_c^0 and Ξ_c^+ baryons and of the branching-fraction ratio $BR(\Xi_c^0 \rightarrow \Xi^- e^+ \nu_e)/BR(\Xi_c^0 \rightarrow \Xi^- \pi^+)$ in pp collisions at $\sqrt{s} = 13$ TeV, *Phys. Rev. Lett.* **127**, 272001 (2021).
- [19] S. Acharya *et al.* (ALICE Collaboration), First measurement of Ω_c^0 production in pp collisions at $\sqrt{s} = 13$ TeV, *Phys. Lett. B* **846**, 137625 (2023).
- [20] A. M. Sirunyan *et al.* (CMS Collaboration), Production of Λ_c^+ baryons in proton-proton and lead-lead collisions at $\sqrt{s_{NN}} = 5.02$ TeV, *Phys. Lett. B* **803**, 135328 (2020).
- [21] A. Tumasyan *et al.* (CMS Collaboration), Study of charm hadronization with prompt Λ_c^+ baryons in proton-proton and lead-lead collisions at $\sqrt{s_{NN}} = 5.02$ TeV, *J. High Energy Phys.* **01** (2024) 128.
- [22] S. Acharya *et al.* (ALICE Collaboration), Charm-quark fragmentation fractions and production cross section at midrapidity in pp collisions at the LHC, *Phys. Rev. D* **105**, L011103 (2022).
- [23] D. Besson *et al.* (CLEO Collaboration), Observation of a narrow resonance of mass 2.46 GeV/ c^2 decaying to $D_s^{*+}\pi^0$ and confirmation of the $D_s^{*+}(2317)$ state, *Phys. Rev. D* **68**, 032002 (2003).
- [24] B. Aubert *et al.* (BABAR Collaboration), Observation of a new D_s meson decaying to DK at a mass of 2.86 GeV/ c^2 , *Phys. Rev. Lett.* **97**, 222001 (2006).
- [25] P. del Amo Sanchez *et al.* (BABAR Collaboration), Observation of new resonances decaying to $D\pi$ and $D^{*+}\pi$ in inclusive e^+e^- collisions near $\sqrt{s} = 10.58$ GeV, *Phys. Rev. D* **82**, 111101 (2010).
- [26] J. Brodzicka *et al.* (Belle Collaboration), Observation of a new D_{sJ} meson in $B^+ \rightarrow \text{anti-}D^0 D^0 K^+$ decays, *Phys. Rev. Lett.* **100**, 092001 (2008).
- [27] J. P. Lees *et al.* (BABAR Collaboration), Dalitz plot analyses of $B^0 \rightarrow D^- D^0 K^+$ and $B^+ \rightarrow \overline{D^0} D^0 K^+$ decays, *Phys. Rev. D* **91**, 052002 (2015).
- [28] R. Aaij *et al.* (LHCb Collaboration), Study of D_{sJ} decays to $D^+ K_S^0$ and $D^0 K^+$ final states in pp collisions, *J. High Energy Phys.* **10** (2012) 151.
- [29] R. Aaij *et al.* (LHCb Collaboration), Study of D_J meson decays to $D^+\pi^-$, $D^0\pi^+$ and $D^{*+}\pi^-$ final states in pp collision, *J. High Energy Phys.* **09** (2013) 145.
- [30] R. Aaij *et al.* (LHCb Collaboration), Amplitude analysis of $B^- \rightarrow D^+\pi^-\pi^-$ decays, *Phys. Rev. D* **94**, 072001 (2016).
- [31] R. Aaij *et al.* (LHCb Collaboration), Dalitz plot analysis of $B^0 \rightarrow \overline{D^0}\pi^+\pi^-$ decays, *Phys. Rev. D* **92**, 032002 (2015).
- [32] K. Ackerstaff *et al.* (OPAL Collaboration), Production of P wave charm and charm-strange mesons in hadronic Z^0 decays, *Z. Phys. C* **76**, 425 (1997).
- [33] A. Heister *et al.* (ALEPH Collaboration), Production of D_s^{**} mesons in hadronic Z decays, *Phys. Lett. B* **526**, 34 (2002).
- [34] S. Chekanov *et al.* (ZEUS Collaboration), Production of excited charm and charm-strange mesons at HERA, *Eur. Phys. J. C* **60**, 25 (2009).
- [35] H. Abramowicz *et al.* (ZEUS Collaboration), Production of the excited charm mesons D_1 and D_2^* at HERA, *Nucl. Phys. B* **866**, 229 (2013).
- [36] A. Andronic, P. Braun-Munzinger, K. Redlich, and J. Stachel, Statistical hadronization of charm in heavy-ion collisions at SPS, RHIC and LHC, *Phys. Lett. B* **571**, 36 (2003).
- [37] M. He and R. Rapp, Charm-baryon production in proton-proton collisions, *Phys. Lett. B* **795**, 117 (2019).
- [38] P. Skands, S. Carrazza, and J. Rojo, Tuning PYTHIA 8.1: The Monash 2013 Tune, *Eur. Phys. J. C* **74**, 3024 (2014).
- [39] S. Acharya *et al.* (ALICE Collaboration), Evidence of rescattering effect in Pb-Pb collisions at the LHC through production of $K^*(892)^0$ and $\phi(1020)$ mesons, *Phys. Lett. B* **802**, 135225 (2020).
- [40] S. Acharya *et al.* (ALICE Collaboration), Multiplicity dependence of $K^*(892)^0$ and $\phi(1020)$ production in pp collisions at $\sqrt{s} = 13$ TeV, *Phys. Lett. B* **807**, 135501 (2020).
- [41] S. Acharya *et al.* (ALICE Collaboration), Measurement of $K^*(892)^\pm$ production in inelastic pp collisions at the LHC, *Phys. Lett. B* **828**, 137013 (2022).
- [42] S. Acharya *et al.* (ALICE Collaboration), $K^*(892)^\pm$ resonance production in Pb-Pb collisions at $\sqrt{s_{NN}} = 5.02$ TeV, *Phys. Rev. C* **109**, 044902 (2024).
- [43] R. L. Workman *et al.* (Particle Data Group), Review of particle physics, *Prog. Theor. Exp. Phys.* **2022**, 083C01 (2022).
- [44] K. Aamodt *et al.* (ALICE Collaboration), The ALICE experiment at the CERN LHC, *J. Instrum.* **3**, S08002 (2008).
- [45] B. Abelev *et al.* (ALICE Collaboration), Performance of the ALICE experiment at the CERN LHC, *Int. J. Mod. Phys. A* **29**, 1430044 (2014).
- [46] S. Acharya *et al.* (ALICE Collaboration), Pseudorapidity distributions of charged particles as a function of mid- and forward rapidity multiplicities in pp collisions at $\sqrt{s} = 5.02, 7$ and 13 TeV, *Eur. Phys. J. C* **81**, 630 (2021).
- [47] S. Acharya *et al.* (ALICE Collaboration), ALICE 2016-2017-2018 luminosity determination for pp collisions at $\sqrt{s} = 13$ TeV, <https://cds.cern.ch/record/2776672>.
- [48] R. Brun, F. Bruyant, F. Carminati, S. Giani, M. Maire, A. McPherson, G. Patrick, and L. Urban, *GEANT: Detector Description and Simulation Tool*; Oct 1994, CERN Program Library (CERN, Geneva, 1993), Long Writeup W5013, <https://cds.cern.ch/record/1082634>.
- [49] S. Acharya *et al.* (ALICE Collaboration), Observation of a multiplicity dependence in the p_T -differential charm baryon-to-meson ratios in proton-proton collisions at $\sqrt{s} = 13$ TeV, *Phys. Lett. B* **829**, 137065 (2022).
- [50] S. Acharya *et al.* (ALICE Collaboration), Production of light-flavor hadrons in pp collisions at $\sqrt{s} = 7$ and $\sqrt{s} = 13$ TeV, *Eur. Phys. J. C* **81**, 256 (2021).
- [51] K. Aamodt *et al.* (ALICE Collaboration), Strange particle production in proton-proton collisions at $\sqrt{s} = 0.9$ TeV with ALICE at the LHC, *Eur. Phys. J. C* **71**, 1594 (2011).

- [52] T. Chen and C. Guestrin, XGBoost: A scalable tree boosting system, in *Proceedings of the 22nd ACM SIGKDD International Conference on Knowledge Discovery and Data Mining, KDD '16* (Association for Computing Machinery, New York, NY, USA, 2016), pp. 785–794, [10.1145/2939672.2939785](https://doi.org/10.1145/2939672.2939785).
- [53] L. Barioglio, F. Catalano, M. Concas, P. Fecchio, F. Grossa, F. Mazzaschi, and M. Puccio, HIPE4ML/HIPE4ML, [10.5281/zenodo.7014886](https://zenodo.7014886) (2022).
- [54] S. Acharya *et al.* (ALICE Collaboration), Measurement of the non-prompt D -meson fraction as a function of multiplicity in proton-proton collisions at $\sqrt{s} = 13$ TeV, *J. High Energy Phys.* **10** (2023) 092.
- [55] S. Acharya *et al.* (ALICE Collaboration), First measurement of prompt and non-prompt D^{*+} vector meson spin alignment in pp collisions at $\sqrt{s} = 13$ TeV, *Phys. Lett. B* **846**, 137920 (2023).
- [56] F. Grossa, S. Politanò, and A. Bigot, FLAREFLY, [10.5281/zenodo.7579657](https://zenodo.7579657) (2023).
- [57] T. Sjöstrand, S. Mrenna, and P. Z. Skands, PYTHIA 6.4 physics and manual, *J. High Energy Phys.* **05** (2006) 026.
- [58] T. Sjöstrand, S. Ask, J. R. Christiansen, R. Corke, N. Desai, P. Ilten, S. Mrenna, S. Prestel, C. O. Rasmussen, and P. Z. Skands, An introduction to PYTHIA 8.2, *Comput. Phys. Commun.* **191**, 159 (2015).
- [59] S. Acharya *et al.* (ALICE Collaboration), Measurement of beauty-quark production in pp collisions at $\sqrt{s} = 13$ TeV via non-prompt D mesons, *J. High Energy Phys.* **10** (2024) 110.
- [60] A. Andronic, P. Braun-Munzinger, M. K. Köhler, A. Mazeliauskas, K. Redlich, J. Stachel, and V. Vislavicius, The multiple-charm hierarchy in the statistical hadronization model, *J. High Energy Phys.* **07** (2021) 035.
- [61] J. Zhao, J. Aichelin, P. B. Gossiaux, and K. Werner, Heavy flavor as a probe of hot QCD matter produced in proton-proton collisions, *Phys. Rev. D* **109**, 054011 (2024).
- [62] K. Werner, Revealing a deep connection between factorization and saturation: New insight into modeling high-energy proton-proton and nucleus-nucleus scattering in the EPOS4 framework, *Phys. Rev. C* **108**, 064903 (2023).
- [63] S. Godfrey and K. Moats, Properties of excited charm and charm-strange mesons, *Phys. Rev. D* **93**, 034035 (2016).
- [64] T. Sjöstrand and M. Utheim, A framework for hadronic rescattering in pp collisions, *Eur. Phys. J. C* **80**, 907 (2020).
- [65] S. Acharya *et al.* (ALICE Collaboration), First study of the two-body scattering involving charm hadrons, *Phys. Rev. D* **106**, 052010 (2022).
- [66] S. Acharya *et al.* (ALICE Collaboration), Studying the interaction between charm and light-flavor mesons, *Phys. Rev. D* **110**, 032004 (2024).
- [67] L. Gladilin, Fragmentation fractions of c and b quarks into charmed hadrons at LEP, *Eur. Phys. J. C* **75**, 19 (2015).
- [68] ALICE Collaboration, <https://www.hepdata.net/record/ins2829721>.

S. Acharya¹²⁷ A. Agarwal¹³⁵ G. Aglieri Rinella¹⁰³² L. Aglietta¹⁰²⁴ M. Agnello¹⁰²⁹ N. Agrawal¹⁰²⁵ Z. Ahmed¹⁰¹³⁵ S. Ahmad¹⁰¹⁵ S. U. Ahn¹⁰⁷¹ I. Ahuja¹⁰³⁷ A. Akindinov¹⁰¹⁴⁰ V. Akishina¹⁰³⁸ M. Al-Turany¹⁰⁹⁷ D. Aleksandrov¹⁰¹⁴⁰ B. Alessandro¹⁰⁵⁶ H. M. Alfanda¹⁰⁶ R. Alfaro Molina¹⁰⁶⁷ B. Ali¹⁰¹⁵ A. Alici¹⁰²⁵ N. Alizadehvandchali¹⁰¹¹⁶ A. Alkin¹⁰¹⁰⁴ J. Alme¹⁰²⁰ G. Alocco¹⁰^{24,52} T. Alt¹⁰⁶⁴ A. R. Altamura¹⁰⁵⁰ I. Altsybeev¹⁰⁹⁵ J. R. Alvarado¹⁰⁴⁴ M. N. Anaam¹⁰⁶ C. Andrei¹⁰⁴⁵ N. Andreou¹⁰¹¹⁵ A. Andronic¹⁰¹²⁶ E. Andronov¹⁰¹⁴⁰ V. Anguelov¹⁰⁹⁴ F. Antinori¹⁰⁵⁴ P. Antonioli¹⁰⁵¹ N. Apadula¹⁰⁷⁴ L. Aphecetche¹⁰¹⁰³ H. Appelhäuser¹⁰⁶⁴ C. Arata¹⁰⁷³ S. Arcelli¹⁰²⁵ R. Arnaldi¹⁰⁵⁶ J. G. M. C. A. Arneiro¹⁰¹¹⁰ I. C. Arsene¹⁰¹⁹ M. Arslanbekci¹⁰¹³⁸ A. Augustinus¹⁰³² R. Averbeck¹⁰⁹⁷ D. Averyanov¹⁰¹⁴⁰ M. D. Azmi¹⁰¹⁵ H. Baba¹⁰¹²⁴ A. Badalà¹⁰⁵³ J. Bae¹⁰¹⁰⁴ Y. W. Baek¹⁰⁴⁰ X. Bai¹⁰¹²⁰ R. Bailhache¹⁰⁶⁴ Y. Bailung¹⁰⁴⁸ R. Bala¹⁰⁹¹ A. Balbino¹⁰²⁹ A. Baldisseri¹⁰¹³⁰ B. Balis¹⁰² Z. Banoo¹⁰⁹¹ V. Barbasova¹⁰³⁷ F. Barile¹⁰³¹ L. Barioglio¹⁰⁵⁶ M. Barlou¹⁰⁷⁸ B. Barman¹⁰⁴¹ G. G. Barnaföldi¹⁰⁴⁶ L. S. Barnby¹⁰¹¹⁵ E. Barreau¹⁰¹⁰³ V. Barret¹⁰¹²⁷ L. Barreto¹⁰¹¹⁰ C. Bartels¹⁰¹¹⁹ K. Barth¹⁰³² E. Bartsch¹⁰⁶⁴ N. Bastid¹⁰¹²⁷ S. Basu¹⁰^{75,a} G. Batigne¹⁰¹⁰³ D. Battistini¹⁰⁹⁵ B. Batyunya¹⁰¹⁴¹ D. Bauri¹⁰⁴⁷ J. L. Bazo Alba¹⁰¹⁰¹ I. G. Bearden¹⁰⁸³ C. Beattie¹⁰¹³⁸ P. Becht¹⁰⁹⁷ D. Behera¹⁰⁴⁸ I. Belikov¹⁰¹²⁹ A. D. C. Bell Hechavarria¹⁰¹²⁶ F. Bellini¹⁰²⁵ R. Bellwied¹⁰¹¹⁶ S. Belokurova¹⁰¹⁴⁰ L. G. E. Beltran¹⁰¹⁰⁹ Y. A. V. Beltran¹⁰⁴⁴ G. Bencedi¹⁰⁴⁶ A. Bensaoula¹⁰¹¹⁶ S. Beole¹⁰²⁴ Y. Berdnikov¹⁰¹⁴⁰ A. Berdnikova¹⁰⁹⁴ L. Bergmann¹⁰⁹⁴ M. G. Besoiu¹⁰⁶³ L. Betev¹⁰³² P. P. Bhaduri¹⁰¹³⁵ A. Bhasin¹⁰⁹¹ B. Bhattacharjee¹⁰⁴¹ L. Bianchi¹⁰²⁴ J. Bielčík¹⁰³⁵ J. Bielčíková¹⁰⁸⁶ A. P. Bigot¹⁰¹²⁹ A. Bilandžić¹⁰⁹⁵ G. Biro¹⁰⁴⁶ S. Biswas¹⁰⁴ N. Bize¹⁰¹⁰³ J. T. Blair¹⁰¹⁰⁸ D. Blau¹⁰¹⁴⁰ M. B. Blidaru¹⁰⁹⁷ N. Bluhme¹⁰³⁸ C. Blume¹⁰⁶⁴ G. Boca¹⁰^{21,55} F. Bock¹⁰⁸⁷ T. Bodova¹⁰²⁰ J. Bok¹⁰¹⁶ L. Boldizsár¹⁰⁴⁶ M. Bombara¹⁰³⁷ P. M. Bond¹⁰³² G. Bonomi¹⁰^{55,134} H. Borel¹⁰¹³⁰ A. Borissov¹⁰¹⁴⁰ A. G. Borquez Carcamo¹⁰⁹⁴ E. Botta¹⁰²⁴ Y. E. M. Bouziani¹⁰⁶⁴ L. Bratrud¹⁰⁶⁴ P. Braun-Munzinger¹⁰⁹⁷ M. Bregant¹⁰¹¹⁰ M. Broz¹⁰³⁵ G. E. Bruno¹⁰^{31,96} V. D. Buchakchiev¹⁰³⁶ M. D. Buckland¹⁰⁸⁵ D. Budnikov¹⁰¹⁴⁰ H. Buesching¹⁰⁶⁴ S. Buflano¹⁰²⁹ P. Buhler¹⁰¹⁰² N. Burmasov¹⁰¹⁴⁰ Z. Buthelezi¹⁰^{68,123} A. Bylinkin¹⁰²⁰ S. A. Bysiak¹⁰¹⁰⁷ J. C. Cabanillas Noris¹⁰¹⁰⁹ M. F. T. Cabrera¹⁰¹¹⁶ M. Cai¹⁰⁶ H. Caines¹⁰¹³⁸ A. Caliva¹⁰²⁸ E. Calvo Villar¹⁰¹⁰¹ J. M. M. Camacho¹⁰¹⁰⁹ P. Camerini¹⁰²³ F. D. M. Canedo¹⁰¹¹⁰ S. L. Cantway¹⁰¹³⁸ M. Carabas¹⁰¹¹³ A. A. Carballo¹⁰³² F. Carnesecchi¹⁰³² R. Caron¹⁰¹²⁸ L. A. D. Carvalho¹⁰¹¹⁰ J. Castillo Castellanos¹⁰¹³⁰ M. Castoldi¹⁰³² F. Catalano¹⁰³² S. Cattaruzzi¹⁰²³

- C. Ceballos Sanchez¹,⁷ R. Cerri¹,²⁴ I. Chakaberia¹,⁷⁴ P. Chakraborty¹,¹³⁶ S. Chandra¹,¹³⁵ S. Chapelard¹,³²
 M. Chartier¹,¹¹⁹ S. Chattopadhyay¹,¹³⁵ S. Chattopadhyay¹,¹³⁵ S. Chattopadhyay¹,⁹⁹ M. Chen,³⁹ T. Cheng¹,⁶
 C. Cheshkov¹,¹²⁸ V. Chibante Barroso¹,³² D. D. Chinellato¹,¹⁰² E. S. Chizzali¹,^{95,b} J. Cho¹,⁵⁸ S. Cho¹,⁵⁸
 P. Chochula¹,³² Z. A. Chochulska¹,¹³⁶ D. Choudhury¹,⁴¹ P. Christakoglou¹,⁸⁴ C. H. Christensen¹,⁸³ P. Christiansen¹,⁷⁵
 T. Chujo¹,¹²⁵ M. Ciacco¹,²⁹ C. Cicalo¹,⁵² M. R. Ciupek¹,⁹⁷ G. Clai,^{51,c} F. Colamaria¹,⁵⁰ J. S. Colburn,¹⁰⁰ D. Colella¹,³¹
 A. Colelli,³¹ M. Coloccia¹,²⁵ M. Concas¹,³² G. Conesa Balbastre¹,⁷³ Z. Conesa del Valle¹,¹³¹ G. Contin¹,²³
 J. G. Contreras¹,³⁵ M. L. Coquet¹,¹⁰³ P. Cortese¹,^{56,133} M. R. Cosentino¹,¹¹² F. Costa¹,³² S. Costanza¹,^{21,55} C. Cot¹,¹³¹
 P. Crochet¹,¹²⁷ M. M. Czarnynoga¹,¹³⁶ A. Dainese¹,⁵⁴ G. Dange,³⁸ M. C. Danisch¹,⁹⁴ A. Danu¹,⁶³ P. Das¹,⁸⁰ S. Das¹,⁴
 A. R. Dash¹,¹²⁶ S. Dash¹,⁴⁷ A. De Caro¹,²⁸ G. de Cataldo¹,⁵⁰ J. de Cuveland,³⁸ A. De Falco¹,²² D. De Gruttola¹,²⁸
 N. De Marco¹,⁵⁶ C. De Martin¹,²³ S. De Pasquale¹,²⁸ R. Deb¹,¹³⁴ R. Del Grande¹,⁹⁵ L. Dello Stritto¹,³² W. Deng¹,⁶
 K. C. Devereaux,¹⁸ P. Dhankher¹,¹⁸ D. Di Bari¹,³¹ A. Di Mauro¹,³² B. Di Ruzza¹,¹³² B. Diab¹,¹³⁰ R. A. Diaz¹,^{7,141}
 T. Dietel¹,¹¹⁴ Y. Ding¹,⁶ J. Ditzel¹,⁶⁴ R. Divià¹,³² Ø. Djupsland¹,²⁰ U. Dmitrieva¹,¹⁴⁰ A. Dobrin¹,⁶³ B. Döningus¹,⁶⁴
 J. M. Dubinski¹,¹³⁶ A. Dubla¹,⁹⁷ P. Dupieux¹,¹²⁷ N. Dzalaiova,¹³ T. M. Eder¹,¹²⁶ R. J. Ehlers¹,⁷⁴ F. Eisenhut¹,⁶⁴
 R. Ejima¹,⁹² D. Elia¹,⁵⁰ B. Erasmus¹,¹⁰³ F. Ercolelli¹,²⁵ B. Espagnon¹,¹³¹ G. Eulisse¹,³² D. Evans¹,¹⁰⁰
 S. Evdokimov¹,¹⁴⁰ L. Fabbietti¹,⁹⁵ M. Faggion¹,²³ J. Faivre¹,⁷³ F. Fan¹,⁶ W. Fan¹,⁷⁴ A. Fantoni¹,⁴⁹ M. Fasel¹,⁸⁷
 A. Feliciello¹,⁵⁶ G. Feofilov¹,¹⁴⁰ A. Fernández Téllez¹,⁴⁴ L. Ferrandi¹,¹¹⁰ M. B. Ferrer¹,³² A. Ferrero¹,¹³⁰
 C. Ferrero¹,^{56,d} A. Ferretti¹,²⁴ V. J. G. Feuillard¹,⁹⁴ V. Filova¹,³⁵ D. Finogeev¹,¹⁴⁰ F. M. Fionda¹,⁵² E. Flatland,³²
 F. Flor¹,^{116,138} A. N. Flores¹,¹⁰⁸ S. Foertsch¹,⁶⁸ I. Fokin¹,⁹⁴ S. Fokin¹,¹⁴⁰ U. Follo¹,^{56,d} E. Fragiocomo¹,⁵⁷ E. Frajna¹,⁴⁶
 U. Fuchs¹,³² N. Funicello¹,²⁸ C. Furget¹,⁷³ A. Furs¹,¹⁴⁰ T. Fusayasu¹,⁹⁸ J. J. Gaardhøje¹,⁸³ M. Gagliardi¹,²⁴
 A. M. Gago¹,¹⁰¹ T. Gahlaut,⁴⁷ C. D. Galvan¹,¹⁰⁹ S. Gami,⁸⁰ D. R. Gangadharan¹,¹¹⁶ P. Ganoti¹,⁷⁸ C. Garabatos¹,⁹⁷
 J. M. Garcia,⁴⁴ T. García Chávez¹,⁴⁴ E. Garcia-Solis¹,⁹ C. Gargiulo¹,³² P. Gasik¹,⁹⁷ H. M. Gaur,³⁸ A. Gautam¹,¹¹⁸
 M. B. Gay Ducati¹,⁶⁶ M. Germain¹,¹⁰³ R. A. Gernhaeuser,⁹⁵ C. Ghosh,¹³⁵ M. Giacalone¹,⁵¹ G. Gioachin¹,²⁹ S. K. Giri,¹³⁵
 P. Giubellino¹,^{56,97} P. Giubilato¹,²⁷ A. M. C. Glaenzer¹,¹³⁰ P. Glässel¹,⁹⁴ E. Glimos¹,¹²² D. J. Q. Goh,⁷⁶ V. Gonzalez¹,¹³⁷
 P. Gordeev¹,¹⁴⁰ M. Gorgon¹,² K. Goswami¹,⁴⁸ S. Gotovac,³³ V. Grabski¹,⁶⁷ L. K. Graczykowski¹,¹³⁶ E. Grecka¹,⁸⁶
 A. Grelli¹,⁵⁹ C. Grigoras¹,³² V. Grigoriev¹,¹⁴⁰ S. Grigoryan¹,^{1,141} F. Grossa¹,³² J. F. Grosse-Oetringhaus¹,³²
 R. Grossi¹,⁹⁷ D. Grund¹,³⁵ N. A. Grunwald,⁹⁴ G. G. Guardiano¹,¹¹¹ R. Guernane¹,⁷³ M. Guilbaud¹,¹⁰³
 K. Gulbrandsen¹,⁸³ J. J. W. K. Gumprecht,¹⁰² T. Gündem¹,⁶⁴ T. Gunji¹,¹²⁴ W. Guo¹,⁶ A. Gupta¹,⁹¹ R. Gupta¹,⁹¹
 R. Gupta¹,⁴⁸ K. Gwizdziel¹,¹³⁶ L. Gyulai¹,⁴⁶ C. Hadjidakis¹,¹³¹ F. U. Haider¹,⁹¹ S. Haidlova¹,³⁵ M. Halder,⁴
 H. Hamagaki¹,⁷⁶ Y. Han¹,¹³⁹ B. G. Hanley¹,¹³⁷ R. Hannigan¹,¹⁰⁸ J. Hansen¹,⁷⁵ M. R. Haque¹,⁹⁷ J. W. Harris¹,¹³⁸
 A. Harton¹,⁹ M. V. Hartung¹,⁶⁴ H. Hassan¹,¹¹⁷ D. Hatzifotiadou¹,⁵¹ P. Hauer¹,⁴² L. B. Havener¹,¹³⁸ E. Hellbär¹,³²
 H. Helstrup¹,³⁴ M. Hemmer¹,⁶⁴ T. Herman¹,³⁵ S. G. Hernandez,¹¹⁶ G. Herrera Corral¹,⁸ S. Herrmann¹,¹²⁸
 K. F. Hetland¹,³⁴ B. Heybeck¹,⁶⁴ H. Hillemanns¹,³² B. Hippolyte¹,¹²⁹ I. P. M. Hobus,⁸⁴ F. W. Hoffmann¹,⁷⁰
 B. Hofman¹,⁵⁹ G. H. Hong¹,¹³⁹ M. Horst¹,⁹⁵ A. Horzyk¹,² Y. Hou¹,⁶ P. Hristov¹,³² P. Huhn,⁶⁴ L. M. Huhta¹,¹¹⁷
 T. J. Humanic¹,⁸⁸ A. Hutson¹,¹¹⁶ D. Hutter¹,³⁸ M. C. Hwang¹,¹⁸ R. Ilkaev¹,¹⁴⁰ M. Inaba¹,¹²⁵ G. M. Innocenti¹,³²
 M. Ippolitov¹,¹⁴⁰ A. Isakov¹,⁸⁴ T. Isidori¹,¹¹⁸ M. S. Islam¹,⁹⁹ S. Iurchenko,¹⁴⁰ M. Ivanov¹,¹³ M. Ivanov,⁹⁷ V. Ivanov¹,¹⁴⁰
 K. E. Iversen¹,⁷⁵ M. Jablonski¹,² B. Jacak¹,^{18,74} N. Jacazio¹,²⁵ P. M. Jacobs¹,⁷⁴ S. Jadlovska,¹⁰⁶ J. Jadlovsky,¹⁰⁶
 S. Jaelani¹,⁸² C. Jahnke¹,¹¹⁰ M. J. Jakubowska¹,¹³⁶ M. A. Janik¹,¹³⁶ T. Janson,⁷⁰ S. Ji¹,¹⁶ S. Jia¹,¹⁰ T. Jiang¹,¹⁰
 A. A. P. Jimenez¹,⁶⁵ F. Jonas¹,⁷⁴ D. M. Jones¹,¹¹⁹ J. M. Jowett¹,^{32,97} J. Jung¹,⁶⁴ M. Jung¹,⁶⁴ A. Junique¹,³²
 A. Jusko¹,¹⁰⁰ J. Kaewjai,¹⁰⁵ P. Kalinak¹,⁶⁰ A. Kalweit¹,³² A. Karasu Uysal¹,^{72,e} D. Karatovic¹,⁸⁹ N. Karatzenis,¹⁰⁰
 O. Karavichev¹,¹⁴⁰ T. Karavicheva¹,¹⁴⁰ E. Karpechev¹,¹⁴⁰ M. J. Karwowska¹,^{32,136} U. Kebschull¹,⁷⁰ M. Keil¹,³²
 B. Ketzer¹,⁴² J. Keul¹,⁶⁴ S. S. Khade¹,⁴⁸ A. M. Khan¹,¹²⁰ S. Khan¹,¹⁵ A. Khanzadeev¹,¹⁴⁰ Y. Kharlov¹,¹⁴⁰
 A. Khatun¹,¹¹⁸ A. Khuntia¹,³⁵ Z. Khuranova¹,⁶⁴ B. Kileng¹,³⁴ B. Kim¹,¹⁰⁴ C. Kim¹,¹⁶ D. J. Kim¹,¹¹⁷ E. J. Kim¹,⁶⁹
 J. Kim¹,¹³⁹ J. Kim¹,⁵⁸ J. Kim¹,^{32,69} M. Kim¹,¹⁸ S. Kim¹,¹⁷ T. Kim¹,¹³⁹ K. Kimura¹,⁹² A. Kirkova,³⁶ S. Kirsch¹,⁶⁴
 I. Kisiel¹,³⁸ S. Kiselev¹,¹⁴⁰ A. Kisiel¹,¹³⁶ J. P. Kitowski¹,² J. L. Klay¹,⁵ J. Klein¹,³² S. Klein¹,⁷⁴ C. Klein-Bösing¹,¹²⁶
 M. Kleiner¹,⁶⁴ T. Klemenz¹,⁹⁵ A. Kluge¹,³² C. Kobdaj¹,¹⁰⁵ R. Kohara,¹²⁴ T. Kollegger,⁹⁷ A. Kondratyev¹,¹⁴¹
 N. Kondratyeva¹,¹⁴⁰ J. Konig¹,⁶⁴ S. A. Konigstorfer¹,⁹⁵ P. J. Konopka¹,³² G. Kornakov¹,¹³⁶ M. Korwieser¹,⁹⁵
 S. D. Koryciak¹,² C. Koster,⁸⁴ A. Kotliarov¹,⁸⁶ N. Kovacic,⁸⁹ V. Kovalenko¹,¹⁴⁰ M. Kowalski¹,¹⁰⁷ V. Kozuharov¹,³⁶
 G. Kozlov,³⁸ I. Králik¹,⁶⁰ A. Kravčáková,³⁷ L. Krcal¹,^{32,38} M. Krivda¹,^{60,100} F. Krizek¹,⁸⁶ K. Krizkova Gajdosova¹,³²
 C. Krug¹,⁶⁶ M. Krüger¹,⁶⁴ D. M. Krupova¹,³⁵ E. Kryshen¹,¹⁴⁰ V. Kučera¹,⁵⁸ C. Kuhn¹,¹²⁹ P. G. Kuijer¹,^{84,a}

- T. Kumaoka,¹²⁵ D. Kumar,¹³⁵ L. Kumar,⁹⁰ N. Kumar,⁹⁰ S. Kumar,⁵⁰ S. Kundu,³² P. Kurashvili,⁷⁹ A. B. Kurepin,¹⁴⁰
 A. Kuryakin,¹⁴⁰ S. Kushpil,⁸⁶ V. Kuskov,¹⁴⁰ M. Kutyla,¹³⁶ A. Kuznetsov,¹⁴¹ M. J. Kweon,⁵⁸ Y. Kwon,¹³⁹
 S. L. La Pointe,³⁸ P. La Rocca,²⁶ A. Lakrathok,¹⁰⁵ M. Lamanna,³² A. R. Landou,⁷³ R. Langoy,¹²¹ P. Larionov,³²
 E. Laudi,³² L. Lautner,^{32,95} R. A. N. Laveaga,¹⁰⁹ R. Lavicka,¹⁰² R. Lea,^{55,134} H. Lee,¹⁰⁴ I. Legrand,⁴⁵
 G. Legras,¹²⁶ J. Lehrbach,³⁸ A. M. Lejeune,³⁵ T. M. Lelek,² R. C. Lemmon,^{85,a} I. León Monzón,¹⁰⁹ M. M. Lesch,⁹⁵
 E. D. Lesser,¹⁸ P. Lévai,⁴⁶ M. Li,⁶ P. Li,¹⁰ X. Li,¹⁰ B. E. Liang-Gilman,¹⁸ J. Lien,¹²¹ R. Lietava,¹⁰⁰ I. Likmeta,¹¹⁶
 B. Lim,²⁴ S. H. Lim,¹⁶ V. Lindenstruth,³⁸ C. Lippmann,⁹⁷ D. H. Liu,⁶ J. Liu,¹¹⁹ G. S. S. Liveraro,¹¹¹
 I. M. Lofnes,²⁰ C. Loizides,⁸⁷ S. Lokos,¹⁰⁷ J. Lömek,⁵⁹ X. Lopez,¹²⁷ E. López Torres,⁷ C. Lotteau,¹²⁸
 P. Lu,^{97,120} Z. Lu,¹⁰ F. V. Lugo,⁶⁷ J. R. Luhder,¹²⁶ M. Lunardon,²⁷ G. Luparello,⁵⁷ Y. G. Ma,³⁹ M. Mager,³²
 A. Maire,¹²⁹ E. M. Majerz,² M. V. Makariev,³⁶ M. Malaev,¹⁴⁰ G. Malfattore,²⁵ N. M. Malik,⁹¹ S. K. Malik,⁹¹
 L. Malinina,^{141,a,f} D. Mallick,¹³¹ N. Mallick,⁴⁸ G. Mandaglio,^{30,53} S. K. Mandal,⁷⁹ A. Manea,⁶³ V. Manko,¹⁴⁰
 F. Manso,¹²⁷ V. Manzari,⁵⁰ Y. Mao,⁶ R. W. Marcjan,² G. V. Margagliotti,²³ A. Margottti,⁵¹ A. Marín,⁹⁷
 C. Markert,¹⁰⁸ C. F. B. Marquez,³¹ P. Martinengo,³² M. I. Martínez,⁴⁴ G. Martínez García,¹⁰³ M. P. P. Martins,¹¹⁰
 S. Masciocchi,⁹⁷ M. Masera,²⁴ A. Masoni,⁵² L. Massacrier,¹³¹ O. Massen,⁵⁹ A. Mastroserio,^{50,132}
 O. Matonoha,⁷⁵ S. Mattiazzo,²⁷ A. Matyja,¹⁰⁷ F. Mazzaschi,^{24,32} M. Mazzilli,¹¹⁶ Y. Melikyan,⁴³ M. Melo,¹¹⁰
 A. Menchaca-Rocha,⁶⁷ J. E. M. Mendez,⁶⁵ E. Meninno,¹⁰² A. S. Menon,¹¹⁶ M. W. Menzel,^{32,94} M. Meres,¹³
 Y. Miake,¹²⁵ L. Micheletti,³² D. Mihai,¹¹³ D. L. Mihaylov,⁹⁵ K. Mikhaylov,^{140,141} N. Minafra,¹¹⁸ D. Miśkowiec,⁹⁷
 A. Modak,¹³⁴ B. Mohanty,⁸⁰ M. Mohisin Khan,^{15,g} M. A. Molander,⁴³ S. Monira,¹³⁶ C. Mordasini,¹¹⁷
 D. A. Moreira De Godoy,¹²⁶ I. Morozov,¹⁴⁰ A. Morsch,³² T. Mrnjavac,³² V. Muccifora,⁴⁹ S. Muhuri,¹³⁵
 J. D. Mulligan,⁷⁴ A. Mulliri,²² M. G. Munhoz,¹¹⁰ R. H. Munzer,⁶⁴ H. Murakami,¹²⁴ S. Murray,¹¹⁴ L. Musa,³²
 J. Musinsky,⁶⁰ J. W. Myrcha,¹³⁶ B. Naik,¹²³ A. I. Nambrath,¹⁸ B. K. Nandi,⁴⁷ R. Nania,⁵¹ E. Nappi,⁵⁰
 A. F. Nassirpour,¹⁷ V. Nastase,¹¹³ A. Nath,⁹⁴ S. Nath,¹³⁵ C. Nattrass,¹²² M. N. Naydenov,³⁶ A. Neagu,¹⁹ A. Negru,¹¹³
 E. Nekrasova,¹⁴⁰ L. Nellen,⁶⁵ R. Nepeivoda,⁷⁵ S. Nese,¹⁹ N. Nicassio,⁵⁰ B. S. Nielsen,⁸³ E. G. Nielsen,⁸³
 S. Nikolaev,¹⁴⁰ S. Nikulin,¹⁴⁰ V. Nikulin,¹⁴⁰ F. Noferini,⁵¹ S. Noh,¹² P. Nomokonov,¹⁴¹ J. Norman,¹¹⁹
 N. Novitzky,⁸⁷ P. Nowakowski,¹³⁶ A. Nyandin,¹⁴⁰ J. Nystrand,²⁰ S. Oh,¹⁷ A. Ohlson,⁷⁵ V. A. Okorokov,¹⁴⁰
 J. Oleniacz,¹³⁶ A. Onnerstad,¹¹⁷ C. Oppedisano,⁵⁶ A. Ortiz Velasquez,⁶⁵ J. Otwinowski,¹⁰⁷ M. Oya,⁹²
 K. Oyama,⁷⁶ Y. Pachmayer,⁹⁴ S. Padhan,⁴⁷ D. Pagano,^{55,134} G. Paić,⁶⁵ S. Paisano-Guzmán,⁴⁴ A. Palasciano,⁵⁰
 I. Panasenko,⁷⁵ S. Panebianco,¹³⁰ C. Pantouvakis,²⁷ H. Park,¹²⁵ H. Park,¹⁰⁴ J. Park,¹²⁵ J. E. Parkkila,³²
 Y. Patley,⁴⁷ R. N. Patra,⁵⁰ B. Paul,¹³⁵ H. Pei,⁶ T. Peitzmann,⁵⁹ X. Peng,¹¹ M. Pennisi,²⁴ S. Perciballi,²⁴
 D. Peresunko,¹⁴⁰ G. M. Perez,⁷ Y. Pestov,¹⁴⁰ M. T. Petersen,⁸³ V. Petrov,¹⁴⁰ M. Petrovici,⁴⁵ S. Piano,⁵⁷ M. Pikna,¹³
 P. Pillot,¹⁰³ O. Pinazza,^{32,51} L. Pinsky,¹¹⁶ C. Pinto,⁹⁵ S. Pisano,⁴⁹ M. Płoskon,⁷⁴ M. Planinic,⁸⁹ F. Pliquet,⁶⁴
 D. K. Plociennik,² M. G. Poghosyan,⁸⁷ B. Polichtchouk,¹⁴⁰ S. Politano,²⁹ N. Poljak,⁸⁹ A. Pop,⁴⁵
 S. Porteboeuf-Houssais,¹²⁷ V. Pozdniakov,^{141,a} I. Y. Pozos,⁴⁴ K. K. Pradhan,⁴⁸ S. K. Prasad,⁴ S. Prasad,⁴⁸
 R. Preghenella,⁵¹ F. Prino,⁵⁶ C. A. Pruneau,¹³⁷ I. Pshenichnov,¹⁴⁰ M. Puccio,³² S. Pucillo,²⁴ S. Qiu,⁸⁴
 L. Quaglia,²⁴ A. M. K. Radhakrishnan,⁴⁸ S. Ragoni,¹⁴ A. Rai,¹³⁸ A. Rakotozafindrabe,¹³⁰ L. Ramello,^{56,133}
 F. Rami,¹²⁹ C. O. Ramírez-Álvarez,⁴⁴ M. Rasa,²⁶ S. S. Räsänen,⁴³ R. Rath,⁵¹ M. P. Rauch,²⁰ I. Ravasenga,³²
 K. F. Read,^{87,122} C. Reckziegel,¹¹² A. R. Redelbach,³⁸ K. Redlich,^{79,h} C. A. Reetz,⁹⁷ H. D. Regules-Medel,⁴⁴
 A. Rehman,²⁰ F. Reidt,³² H. A. Reme-Ness,³⁴ K. Reygers,⁹⁴ A. Riabov,¹⁴⁰ V. Riabov,¹⁴⁰ R. Ricci,²⁸
 M. Richter,²⁰ A. A. Riedel,⁹⁵ W. Riegler,³² A. G. Riffero,²⁴ M. Rignanese,²⁷ C. Ripoli,²⁸ C. Ristea,⁶³
 M. V. Rodriguez,³² M. Rodríguez Cahuantzi,⁴⁴ S. A. Rodríguez Ramírez,⁴⁴ K. Røed,¹⁹ R. Rogalev,¹⁴⁰
 E. Rogochaya,¹⁴¹ T. S. Rogoschinski,⁶⁴ D. Rohr,³² D. Röhrich,²⁰ S. Rojas Torres,³⁵ P. S. Rokita,¹³⁶
 G. Romanenko,²⁵ F. Ronchetti,³² E. D. Rosas,⁶⁵ K. Roslon,¹³⁶ A. Rossi,⁵⁴ A. Roy,⁴⁸ S. Roy,⁴⁷ N. Rubini,^{25,51}
 J. A. Rudolph,⁸⁴ D. Ruggiano,¹³⁶ R. Rui,²³ P. G. Russek,² R. Russo,⁸⁴ A. Rustamov,⁸¹ E. Ryabinkin,¹⁴⁰
 Y. Ryabov,¹⁴⁰ A. Rybicki,¹⁰⁷ J. Ryu,¹⁶ W. Rzesz,¹³⁶ B. Sabiu,⁵¹ S. Sadovsky,¹⁴⁰ J. Saetre,²⁰ K. Šafařík,³⁵
 S. Saha,⁸⁰ B. Sahoo,⁴⁸ R. Sahoo,⁴⁸ S. Sahoo,⁶¹ D. Sahu,⁴⁸ P. K. Sahu,⁶¹ J. Saini,¹³⁵ K. Sajdakova,³⁷ S. Sakai,¹²⁵
 M. P. Salvan,⁹⁷ S. Sambyal,⁹¹ D. Samitz,¹⁰² I. Sanna,^{32,95} T. B. Saramela,¹¹⁰ D. Sarkar,⁸³ P. Sarma,⁴¹
 V. Sarritzu,²² V. M. Sarti,⁹⁵ M. H. P. Sas,³² S. Sawan,⁸⁰ E. Scapparone,⁵¹ J. Schambach,⁸⁷ H. S. Scheid,⁶⁴
 C. Schiaua,⁴⁵ R. Schicker,⁹⁴ F. Schlepper,⁹⁴ A. Schmah,⁹⁷ C. Schmidt,⁹⁷ H. R. Schmidt,⁹³ M. O. Schmidt,³²
 M. Schmidt,⁹³ N. V. Schmidt,⁸⁷ A. R. Schmier,¹²² R. Schotter,^{102,129} A. Schröter,³⁸ J. Schukraft,³² K. Schweda,⁹⁷

- G. Sciolli²⁵, E. Scomparin⁵⁶, J. E. Seger¹⁴, Y. Sekiguchi¹²⁴, D. Sekihata¹²⁴, M. Selina⁸⁴, I. Selyuzhenkov⁹⁷, S. Senyukov¹²⁹, J. J. Seo⁹⁴, D. Serebryakov¹⁴⁰, L. Serkin⁶⁵, L. Šerkšnytė⁹⁵, A. Sevcenco⁶³, T. J. Shaba⁶⁸, A. Shabetai¹⁰³, R. Shahoyan³², A. Shangaraev¹⁴⁰, B. Sharma⁹¹, D. Sharma⁴⁷, H. Sharma⁵⁴, M. Sharma⁹¹, S. Sharma⁷⁶, S. Sharma⁹¹, U. Sharma⁹¹, A. Shatat¹³¹, O. Sheibani¹¹⁶, K. Shigaki⁹², M. Shimomura⁷⁷, J. Shin¹², S. Shirinkin¹⁴⁰, Q. Shou³⁹, Y. Sibirjak¹⁴⁰, S. Siddhanta⁵², T. Siemiarczuk⁷⁹, T. F. Silva¹¹⁰, D. Silvermyr⁷⁵, T. Simantathammakul¹⁰⁵, R. Simeonov³⁶, B. Singh⁹¹, B. Singh⁹⁵, K. Singh⁴⁸, R. Singh⁸⁰, R. Singh⁹¹, R. Singh⁹⁷, S. Singh¹⁵, V. K. Singh¹³⁵, V. Singhal¹³⁵, T. Sinha⁹⁹, B. Sitar¹³, M. Sitta^{56,133}, T. B. Skaali¹⁹, G. Skorodumovs⁹⁴, N. Smirnov¹³⁸, R. J. M. Snellings⁵⁹, E. H. Solheim¹⁹, J. Song¹⁶, C. Sonnabend^{32,97}, J. M. Sonneveld⁸⁴, F. Soramel²⁷, A. B. Soto-Hernandez⁸⁸, R. Spijkers⁸⁴, I. Sputowska¹⁰⁷, J. Staa⁷⁵, J. Stachel⁹⁴, I. Stan⁶³, P. J. Steffanic¹²², T. Stellhorn¹²⁶, S. F. Stiebelmaier⁹⁴, D. Stocco¹⁰³, I. Storehaug¹⁹, N. J. Strangmann⁶⁴, P. Stratmann¹²⁶, S. Strazzi²⁵, A. Sturniolo^{30,53}, C. P. Stylianidis⁸⁴, A. A. P. Suaide¹¹⁰, C. Suire¹³¹, M. Sukhanov¹⁴⁰, M. Suljic³², R. Sultanov¹⁴⁰, V. Sumberia⁹¹, S. Sumowidagdo⁸², M. Szymkowski¹³⁶, S. F. Taghavi⁹⁵, G. Taillepied⁹⁷, J. Takahashi¹¹¹, G. J. Tambave⁸⁰, S. Tang⁶, Z. Tang¹²⁰, J. D. Tapia Takaki¹¹⁸, N. Tapus¹¹³, L. A. Tarasovicova³⁷, M. G. Tarzila⁴⁵, G. F. Tassielli³¹, A. Tauro³², A. Tavira García¹³¹, G. Tejeda Muñoz⁴⁴, L. Terlizzi²⁴, C. Terrevoli⁵⁰, S. Thakur⁴, D. Thomas¹⁰⁸, A. Tikhonov¹⁴⁰, N. Tiltmann^{32,126}, A. R. Timmins¹¹⁶, M. Tkacik¹⁰⁶, T. Tkacik¹⁰⁶, A. Toia⁶⁴, R. Tokumoto⁹², S. Tomassini²⁵, K. Tomohiro⁹², N. Topilskaya¹⁴⁰, M. Toppi⁴⁹, V. V. Torres¹⁰³, A. G. Torres Ramos³¹, A. Trifiró^{30,53}, T. Triloki⁹⁶, A. S. Triolo^{30,32,53}, S. Tripathy³², T. Tripathy⁴⁷, S. Trogolo²⁴, V. Trubnikov³, W. H. Trzaska¹¹⁷, T. P. Trzcinski¹³⁶, C. Tsolanta¹⁹, R. Tu³⁹, A. Tumkin¹⁴⁰, R. Turrisi⁵⁴, T. S. Tveter¹⁹, K. Ullaland²⁰, B. Ulukutlu⁹⁵, S. Upadhyaya¹⁰⁷, A. Uras¹²⁸, M. Urioni¹³⁴, G. L. Usai²², M. Vala³⁷, N. Valle⁵⁵, L. V. R. van Doremalen⁵⁹, M. van Leeuwen⁸⁴, C. A. van Veen⁹⁴, R. J. G. van Weelden⁸⁴, P. Vande Vyvre³², D. Varga⁴⁶, Z. Varga⁴⁶, P. Vargas Torres⁶⁵, M. Vasileiou⁷⁸, A. Vasiliev^{140,a}, O. Vázquez Doce⁴⁹, O. Vázquez Rueda¹¹⁶, V. Vechernin¹⁴⁰, E. Vercellin²⁴, S. Vergara Limón⁴⁴, R. Verma⁴⁷, L. Vermunt⁹⁷, R. Vértesi⁴⁶, M. Verweij⁵⁹, L. Vickovic³³, Z. Vilakazi¹²³, O. Villalobos Baillie¹⁰⁰, A. Villani²³, A. Vinogradov¹⁴⁰, T. Virgili²⁸, M. M. O. Virta¹¹⁷, A. Vodopyanov¹⁴¹, B. Volkel³², M. A. Völkli⁹⁴, S. A. Voloshin¹³⁷, G. Volpe³¹, B. von Haller³², I. Vorobyev³², N. Vozniuk¹⁴⁰, J. Vrláková³⁷, J. Wan³⁹, C. Wang³⁹, D. Wang³⁹, Y. Wang³⁹, Y. Wang⁶, Z. Wang³⁹, A. Wegrzynek³², F. T. Weiglhofer³⁸, S. C. Wenzel³², J. P. Wessels¹²⁶, J. Wiechula⁶⁴, J. Wikne¹⁹, G. Wilk⁷⁹, J. Wilkinson⁹⁷, G. A. Willems¹²⁶, B. Windelband⁹⁴, M. Winn¹³⁰, J. R. Wright¹⁰⁸, W. Wu³⁹, Y. Wu¹²⁰, Z. Xiong¹²⁰, R. Xu⁶, A. Yadav⁴², A. K. Yadav¹³⁵, Y. Yamaguchi⁹², S. Yang²⁰, S. Yano⁹², E. R. Yeats¹⁸, Z. Yin⁶, I.-K. Yoo¹⁶, J. H. Yoon⁵⁸, H. Yu¹², S. Yuan²⁰, A. Yuncu⁹⁴, V. Zaccolo²³, C. Zampolli³², F. Zanone⁹⁴, N. Zardoshti³², A. Zarochentsev¹⁴⁰, P. Závada⁶², N. Zavyalov¹⁴⁰, M. Zhalov¹⁴⁰, B. Zhang^{6,94}, C. Zhang¹³⁰, L. Zhang³⁹, M. Zhang^{6,127}, M. Zhang⁶, S. Zhang³⁹, X. Zhang⁶, Y. Zhang¹²⁰, Z. Zhang⁶, M. Zhao¹⁰, V. Zhrebchevskii¹⁴⁰, Y. Zhi¹⁰, D. Zhou⁶, Y. Zhou⁸³, J. Zhu^{6,54}, S. Zhu¹²⁰, Y. Zhu⁶, S. C. Zugravel⁵⁶ and N. Zurlo^{55,134}

(ALICE Collaboration)

¹A.I. Alikhanyan National Science Laboratory (Yerevan Physics Institute) Foundation, Yerevan, Armenia²AGH University of Krakow, Cracow, Poland³Bogolyubov Institute for Theoretical Physics, National Academy of Sciences of Ukraine, Kiev, Ukraine⁴Bose Institute, Department of Physics and Centre for Astroparticle Physics and Space Science (CAPSS), Kolkata, India⁵California Polytechnic State University, San Luis Obispo, California, United States⁶Central China Normal University, Wuhan, China⁷Centro de Aplicaciones Tecnológicas y Desarrollo Nuclear (CEADEN), Havana, Cuba⁸Centro de Investigación y de Estudios Avanzados (CINVESTAV), Mexico City and Mérida, Mexico⁹Chicago State University, Chicago, Illinois, USA¹⁰China Institute of Atomic Energy, Beijing, China¹¹China University of Geosciences, Wuhan, China¹²Chungbuk National University, Cheongju, Republic of Korea¹³Comenius University Bratislava, Faculty of Mathematics, Physics and Informatics, Bratislava, Slovak Republic¹⁴Creighton University, Omaha, Nebraska, USA

- ¹⁵Department of Physics, Aligarh Muslim University, Aligarh, India
¹⁶Department of Physics, Pusan National University, Pusan, Republic of Korea
¹⁷Department of Physics, Sejong University, Seoul, Republic of Korea
¹⁸Department of Physics, University of California, Berkeley, California, USA
¹⁹Department of Physics, University of Oslo, Oslo, Norway
²⁰Department of Physics and Technology, University of Bergen, Bergen, Norway
²¹Dipartimento di Fisica, Università di Pavia, Pavia, Italy
²²Dipartimento di Fisica dell'Università and Sezione INFN, Cagliari, Italy
²³Dipartimento di Fisica dell'Università and Sezione INFN, Trieste, Italy
²⁴Dipartimento di Fisica dell'Università and Sezione INFN, Turin, Italy
²⁵Dipartimento di Fisica e Astronomia dell'Università and Sezione INFN, Bologna, Italy
²⁶Dipartimento di Fisica e Astronomia dell'Università and Sezione INFN, Catania, Italy
²⁷Dipartimento di Fisica e Astronomia dell'Università and Sezione INFN, Padova, Italy
²⁸Dipartimento di Fisica 'E.R. Caianiello' dell'Università and Gruppo Collegato INFN, Salerno, Italy
²⁹Dipartimento DISAT del Politecnico and Sezione INFN, Turin, Italy
³⁰Dipartimento di Scienze MIFT, Università di Messina, Messina, Italy
³¹Dipartimento Interateneo di Fisica "M. Merlin" and Sezione INFN, Bari, Italy
³²European Organization for Nuclear Research (CERN), Geneva, Switzerland
³³Faculty of Electrical Engineering, Mechanical Engineering and Naval Architecture, University of Split, Split, Croatia
³⁴Faculty of Engineering and Science, Western Norway University of Applied Sciences, Bergen, Norway
³⁵Faculty of Nuclear Sciences and Physical Engineering, Czech Technical University in Prague, Prague, Czech Republic
³⁶Faculty of Physics, Sofia University, Sofia, Bulgaria
³⁷Faculty of Science, P.J. Šafárik University, Košice, Slovak Republic
³⁸Frankfurt Institute for Advanced Studies, Johann Wolfgang Goethe-Universität Frankfurt, Frankfurt, Germany
³⁹Fudan University, Shanghai, China
⁴⁰Gangneung-Wonju National University, Gangneung, Republic of Korea
⁴¹Gauhati University, Department of Physics, Guwahati, India
⁴²Helmholtz-Institut für Strahlen- und Kernphysik, Rheinische Friedrich-Wilhelms-Universität Bonn, Bonn, Germany
⁴³Helsinki Institute of Physics (HIP), Helsinki, Finland
⁴⁴High Energy Physics Group, Universidad Autónoma de Puebla, Puebla, Mexico
⁴⁵Horia Hulubei National Institute of Physics and Nuclear Engineering, Bucharest, Romania
⁴⁶HUN-REN Wigner Research Centre for Physics, Budapest, Hungary
⁴⁷Indian Institute of Technology Bombay (IIT), Mumbai, India
⁴⁸Indian Institute of Technology Indore, Indore, India
⁴⁹INFN, Laboratori Nazionali di Frascati, Frascati, Italy
⁵⁰INFN, Sezione di Bari, Bari, Italy
⁵¹INFN, Sezione di Bologna, Bologna, Italy
⁵²INFN, Sezione di Cagliari, Cagliari, Italy
⁵³INFN, Sezione di Catania, Catania, Italy
⁵⁴INFN, Sezione di Padova, Padova, Italy
⁵⁵INFN, Sezione di Pavia, Pavia, Italy
⁵⁶INFN, Sezione di Torino, Turin, Italy
⁵⁷INFN, Sezione di Trieste, Trieste, Italy
⁵⁸Inha University, Incheon, Republic of Korea
⁵⁹Institute for Gravitational and Subatomic Physics (GRASP), Utrecht University/Nikhef, Utrecht, Netherlands
⁶⁰Institute of Experimental Physics, Slovak Academy of Sciences, Košice, Slovak Republic
⁶¹Institute of Physics, Homi Bhabha National Institute, Bhubaneswar, India
⁶²Institute of Physics of the Czech Academy of Sciences, Prague, Czech Republic
⁶³Institute of Space Science (ISS), Bucharest, Romania
⁶⁴Institut für Kernphysik, Johann Wolfgang Goethe-Universität Frankfurt, Frankfurt, Germany
⁶⁵Instituto de Ciencias Nucleares, Universidad Nacional Autónoma de México, Mexico City, Mexico
⁶⁶Instituto de Física, Universidade Federal do Rio Grande do Sul (UFRGS), Porto Alegre, Brazil
⁶⁷Instituto de Física, Universidad Nacional Autónoma de México, Mexico City, Mexico
⁶⁸iThemba LABS, National Research Foundation, Somerset West, South Africa
⁶⁹Jeonbuk National University, Jeonju, Republic of Korea

- ⁷⁰Johann-Wolfgang-Goethe Universität Frankfurt Institut für Informatik,
Fachbereich Informatik und Mathematik, Frankfurt, Germany
- ⁷¹Korea Institute of Science and Technology Information, Daejeon, Republic of Korea
- ⁷²KTO Karatay University, Konya, Turkey
- ⁷³Laboratoire de Physique Subatomique et de Cosmologie, Université Grenoble-Alpes, CNRS-IN2P3,
Grenoble, France
- ⁷⁴Lawrence Berkeley National Laboratory, Berkeley, California, USA
- ⁷⁵Lund University Department of Physics, Division of Particle Physics, Lund, Sweden
- ⁷⁶Nagasaki Institute of Applied Science, Nagasaki, Japan
- ⁷⁷Nara Women's University (NWU), Nara, Japan
- ⁷⁸National and Kapodistrian University of Athens, School of Science, Department of Physics,
Athens, Greece
- ⁷⁹National Centre for Nuclear Research, Warsaw, Poland
- ⁸⁰National Institute of Science Education and Research, Homi Bhabha National Institute, Jatni, India
- ⁸¹National Nuclear Research Center, Baku, Azerbaijan
- ⁸²National Research and Innovation Agency—BRIN, Jakarta, Indonesia
- ⁸³Niels Bohr Institute, University of Copenhagen, Copenhagen, Denmark
- ⁸⁴Nikhef, National institute for subatomic physics, Amsterdam, Netherlands
- ⁸⁵Nuclear Physics Group, STFC Daresbury Laboratory, Daresbury, United Kingdom
- ⁸⁶Nuclear Physics Institute of the Czech Academy of Sciences, Husinec-Řež, Czech Republic
- ⁸⁷Oak Ridge National Laboratory, Oak Ridge, Tennessee, United States
- ⁸⁸Ohio State University, Columbus, Ohio, USA
- ⁸⁹Physics department, Faculty of science, University of Zagreb, Zagreb, Croatia
- ⁹⁰Physics Department, Panjab University, Chandigarh, India
- ⁹¹Physics Department, University of Jammu, Jammu, India
- ⁹²Physics Program and International Institute for Sustainability with Knotted Chiral Meta Matter
(SKCM2), Hiroshima University, Hiroshima, Japan
- ⁹³Physikalisches Institut, Eberhard-Karls-Universität Tübingen, Tübingen, Germany
- ⁹⁴Physikalisches Institut, Ruprecht-Karls-Universität Heidelberg, Heidelberg, Germany
- ⁹⁵Physik Department, Technische Universität München, Munich, Germany
- ⁹⁶Politecnico di Bari and Sezione INFN, Bari, Italy
- ⁹⁷Research Division and ExtreMe Matter Institute EMMI, GSI Helmholtzzentrum für
Schwerionenforschung GmbH, Darmstadt, Germany
- ⁹⁸Saga University, Saga, Japan
- ⁹⁹Saha Institute of Nuclear Physics, Homi Bhabha National Institute, Kolkata, India
- ¹⁰⁰School of Physics and Astronomy, University of Birmingham, Birmingham, United Kingdom
- ¹⁰¹Sección Física, Departamento de Ciencias, Pontificia Universidad Católica del Perú, Lima, Peru
- ¹⁰²Stefan Meyer Institut für Subatomare Physik (SMI), Vienna, Austria
- ¹⁰³SUBATECH, IMT Atlantique, Nantes Université, CNRS-IN2P3, Nantes, France
- ¹⁰⁴Sungkyunkwan University, Suwon City, Republic of Korea
- ¹⁰⁵Suranaree University of Technology, Nakhon Ratchasima, Thailand
- ¹⁰⁶Technical University of Košice, Košice, Slovak Republic
- ¹⁰⁷The Henryk Niewodniczanski Institute of Nuclear Physics, Polish Academy of Sciences, Cracow, Poland
- ¹⁰⁸The University of Texas at Austin, Austin, Texas, USA
- ¹⁰⁹Universidad Autónoma de Sinaloa, Culiacán, Mexico
- ¹¹⁰Universidade de São Paulo (USP), São Paulo, Brazil
- ¹¹¹Universidade Estadual de Campinas (UNICAMP), Campinas, Brazil
- ¹¹²Universidade Federal do ABC, Santo André, Brazil
- ¹¹³Universitatea Națională de Știință și Tehnologie Politehnica București, Bucharest, Romania
- ¹¹⁴University of Cape Town, Cape Town, South Africa
- ¹¹⁵University of Derby, Derby, United Kingdom
- ¹¹⁶University of Houston, Houston, Texas, USA
- ¹¹⁷University of Jyväskylä, Jyväskylä, Finland
- ¹¹⁸University of Kansas, Lawrence, Kansas, USA
- ¹¹⁹University of Liverpool, Liverpool, United Kingdom
- ¹²⁰University of Science and Technology of China, Hefei, China
- ¹²¹University of South-Eastern Norway, Kongsberg, Norway
- ¹²²University of Tennessee, Knoxville, Tennessee, USA

- ¹²³*University of the Witwatersrand, Johannesburg, South Africa*
¹²⁴*University of Tokyo, Tokyo, Japan*
¹²⁵*University of Tsukuba, Tsukuba, Japan*
¹²⁶*Universität Münster, Institut für Kernphysik, Münster, Germany*
¹²⁷*Université Clermont Auvergne, CNRS/IN2P3, LPC, Clermont-Ferrand, France*
¹²⁸*Université de Lyon, CNRS/IN2P3, Institut de Physique des 2 Infinis de Lyon, Lyon, France*
¹²⁹*Université de Strasbourg, CNRS, IPHC UMR 7178, F-67000 Strasbourg, France, Strasbourg, France*
¹³⁰*Université Paris-Saclay, Centre d'Etudes de Saclay (CEA), IRFU, Département de Physique Nucléaire (DPN), Saclay, France*
¹³¹*Université Paris-Saclay, CNRS/IN2P3, IJCLab, Orsay, France*
¹³²*Università degli Studi di Foggia, Foggia, Italy*
¹³³*Università del Piemonte Orientale, Vercelli, Italy*
¹³⁴*Università di Brescia, Brescia, Italy*
¹³⁵*Variable Energy Cyclotron Centre, Homi Bhabha National Institute, Kolkata, India*
¹³⁶*Warsaw University of Technology, Warsaw, Poland*
¹³⁷*Wayne State University, Detroit, Michigan, USA*
¹³⁸*Yale University, New Haven, Connecticut, USA*
¹³⁹*Yonsei University, Seoul, Republic of Korea*
¹⁴⁰*Affiliated with an institute covered by a cooperation agreement with CERN*
¹⁴¹*Affiliated with an international laboratory covered by a cooperation agreement with CERN*

^aDeceased.

^bAlso at Max-Planck-Institut fur Physik, Munich, Germany.

^cAlso at Italian National Agency for New Technologies, Energy and Sustainable Economic Development (ENEA), Bologna, Italy.

^dAlso at Dipartimento DET del Politecnico di Torino, Turin, Italy.

^eAlso at Yildiz Technical University, Istanbul, Türkiye.

^fAlso at An institution covered by a cooperation agreement with CERN.

^gAlso at Department of Applied Physics, Aligarh Muslim University, Aligarh, India.

^hAlso at Institute of Theoretical Physics, University of Wroclaw, Poland.